Effects of locally administered bisphosphonate and rhBMP-2 on bone regeneration in the rat fibula

Eun-Jung Kwak

The Graduate School

Yonsei University

Department of Dentistry

Effects of locally administered bisphosphonate and rhBMP-2 on bone regeneration in the rat fibula

Directed by Professor Hyung Jun Kim

A Dissertation Thesis
Submitted to the Department of Dentistry
and the Graduate School of Yonsei University
in partial fulfillment of the
requirements for the degree of
Doctor of Philosophy in Dental Science

Eun-Jung Kwak

June 2016

연세대학교
YONSEI UNIVERSITY

This certifies that the Doctoral Dissertation

of Eun-Jung Kwak is approved.

Thesis Supervisor: Hyung Jun Kim

In-Ho Cha

Woong Nam

Jong In Yook

Young-Bum Park

The Graduate School
Yonsei University

June 2016

감사의 글

구강악안면외과 의사로서 자부심을 가지고 의술을 바르게 행할 수 있게 세심한 지도와 아낌 없는 격려를 주신 김형준 지도 교수님께 가장 먼저 감사를 드립니다. 또한 바쁘신 중에도 논문 심사를 맡아주시고 관심과 조언을 주신 차인호 교수님, 남웅 교수님, 육종인 교수님, 박영범 교수님께도 마음 깊이 감사 드립니다.

치과 영역의 최후방 전선에서 흔들리지 않고 올바르게 성장해 나갈 수 있도록 이끌어 주신 박형식 교수님, 이상휘 교수님, 강정완 교수님, 정영수 교수님, 정휘동 교수님께도 존경과 깊은 감사를 드립니다.

이 논문이 완성되기까지 도움을 주신 백지웅 선배님, 수련생활 동한 함께하며 힘이 되어준 김동욱, 김준영, 김진근, 김현영 그리고 의국 선배님들과 후배들께도 감사의 마음을 전합니다.

지금의 제가 있게 해주시고 언제나 곁에서 제 편이 되어주시는 사랑하는 부모님과 동생 현정에게도 항상 감사하다는 말을 전하고 싶습니다. 늘 겸손한 자세로 끊임없이 정진하는 구강악안면외과 의사가 되도록 노력하겠습니다. 감사합니다.

2016년 6월

곽 은 정

TABLE OF CONTENTS

LIST OF FIGURES ····· iii

LIST OF TABLES ····· vi

ABSTRACT ····· vii

1. Introduction ····· 1

2. Materials and Methods ····· 3

2.1. Animals ····· 3

2.2. Experimental design ····· 3

2.2.1. Experiment 1 ····· 3

2.2.2. Experiment 2 ····· 5

2.3. Surgical procedure ····· 7

2.4. Assessment methods ····· 10

2.4.1. Plain radiographic evaluation ····· 10

2.4.2. Micro-computed tomography (micro-CT) ····· 10

2.4.3. Histology and histomorphometry ····· 11

2.4.4. Immunohistochemistry ····· 14

2.5. Statistical analysis ····· 14

3. Results ····· 15

3.1. Gross examination ····· 15

3.1.1. Experiment 1 ····· 15
3.1.2. Experiment 2 ····· 15
3.2. Radiographic evaluation ····· 16
3.2.1. Experiment 1 ····· 16
3.2.2. Experiment 2 ····· 18
3.3. Micro-CT evaluation ····· 20
3.3.1. Experiment 1 ····· 20
3.3.2. Experiment 2 ····· 27
3.4. Statistical analysis of micro-CT data ····· 34
3.5. Histological findings ····· 38
3.5.1. Experiment 1 ····· 38
3.5.2. Experiment 2 ····· 41
3.6. Histomorphometric analysis ····· 44
3.7. Immunohistochemical findings ····· 45
4. Discussion ····· 48
5. Conclusion ····· 53
6. References ····· 54
ABSTRACT (in Korean) ····· 57

LIST OF FIGURES

Figure 1. Schematic study design of experiment 1 ····· 5

Figure 2. Schematic study design of experiment 2 ····· 6

Figure 3. Inhalation anesthesia instruments ····· 8

Figure 4. Procedure of alendronate or rhBMP-2 loaded CollaOss® or Rapiderm pad® graft9

Figure 5. The selected area of resection margin and graft analyzed in histomorphometry ····· 12

Figure 6. Measurement of bone material, newly formed bone, adipose tissue by Adobe Photoshop CS4 ····· 12

Figure 7. The selection of area and measuring thickness of cortical layer ····· 13

Figure 8. Radiographic findings (Plain x-ray) of 4-week experimental group 1 on left and right side ····· 17

Figure 9. Radiographic findings (Plain x-ray) of 8-week experimental group 1 on left and right side ····· 17

Figure 10. Radiographic findings (Plain x-ray) of 4-week experimental group 2 on left and right side ····· 19

Figure 11. Radiographic findings (Plain x-ray) of 8-week experimental group 2 on left and right side ····· 19

Figure 12. 3-dimensional reconstruction image, Long axis CT view of 4-week left fibula

in experiment 1 ····· 22

Figure 13. The rate of CT, NB, BM of experimental group 1 ····· 23

Figure 14. 3-dimensional reconstruction image, Long axis CT view of 4-week right fibula in experiment 1 ····· 24

Figure 15. 3-dimensional reconstruction image, Long axis CT view of 8-week left fibula in experiment 1 ····· 25

Figure 16. 3-dimensional reconstruction image, Long axis CT view of 8-week right fibula in experiment 1 ····· 26

Figure 17. 3-dimensional reconstruction image, Long axis CT view of 4-week left fibula in experiment 2 ····· 29

Figure 18. The rate of CT, NB, BM of experimental group 2 ····· 30

Figure 19. 3-dimensional reconstruction image, Long axis CT view of 4-week right fibula in experiment 2 ····· 31

Figure 20. 3-dimensional reconstruction image, Long axis CT view of 8-week left fibula in experiment 2 ····· 32

Figure 21. 3-dimensional reconstruction image, Long axis CT view of 8-week right fibula in experiment 2 ····· 33

Figure 22. The rate of CT, NB, BM of 4-week experimental group ····· 34

Figure 23. The rate of CT, NB, BM of 8-week experimental group ····· 35

Figure 24. The rate of CT, NB, BM of 4 and 8-week experimental group ····· 36

Figure 25. Histologic findings of 4-week left fibula in experiment 1 ····· 39

Figure 26. Histologic findings of 4-week right fibula in experiment 1 ····· 39

Figure 27. Histologic findings of 8-week left fibula in experiment 1 ····· 40

Figure 28. Histologic findings of 8-week right fibula in experiment 1 ····· 40

Figure 29. Histologic findings of 4-week left fibula in experiment 2 ····· 42

Figure 30. Histologic findings of 4-week right fibula in experiment 2 ····· 42

Figure 31. Histologic findings of 8-week left fibula in experiment 2 ····· 43

Figure 32. Histologic findings of 8-week right fibula in experiment 2 ····· 43

Figure 33. The rate of CT, AP, NB, BM of 8-week experimental group ····· 44

Figure 34. The thickness of cortical layer of 8-week experimental group ····· 45

Figure 35. Immunohistochemical findings with BMP2 of experimental group 1 ····· 46

Figure 36. Immunohistochemical findings with BMP2 of experimental group 2 ····· 46

Figure 37. Immunohistochemical findings with OPG of experimental group 1 ····· 47

Figure 38. Immunohistochemical findings with OPG of experimental group 2 ····· 47

LIST OF TABLES

Table 1. Study design of experiment 1 ····· 4

Table 2. Study design of experiment 2 ····· 6

Table 3. Statistical analysis of 4-week experimental group ····· 37

Table 4. Statistical analysis of 8-week experimental group ····· 37

Table 5. Statistical analysis of 4 and 8-week experimental group ····· 37

Table 6. Statistical analysis of ALN(H) and BMP(C) group ····· 37

ABSTRACT

Effects of locally administered bisphosphonate and rhBMP-2 on bone regeneration in the rat fibula

Eun-Jung Kwak

Department of Dentistry
The Graduate School, Yonsei University
(Directed by Professor Hyung Jun Kim, DDS, PhD)

The mechanism of bone formation involves osteogenesis, osteoinduction, and osteoconduction. Autogenous bone is the most useful graft material because of its osteogenic and osteoinductive features. For large defects caused by tumors or trauma, which are commonly encountered in oral and maxillofacial surgery, xenografting or allografting is required. However, these methods may not be sufficient because they only facilitate osteoconduction. In addition to studies of bone graft material, osteoinductive factors, such as recombinant human bone morphogenetic protein-2 (rhBMP-2), have also been investigated. For new bone formation, bone forming factors and carriers are both important; however, no studies have investigated appropriate carriers for rhBMP-2. Importantly, recent studies have demonstrated the anabolic effects of locally administered

bisphosphonate, which affects both osteoclasts and osteoblasts. Thus, in this study, we evaluated the ability of CollaOss (xenogenic bone) and Rapiderm Pad (absorbable collagen sponge) to function as an rhBMP-2 carrier. Furthermore, the osteoinductive ability of bisphosphonate was studied by comparison with rhBMP-2. Thirty-two Sprague-Dawley male rats were divided into two groups to study the bone-forming ability of bisphosphonate and to identify an appropriate carrier for rhBMP-2. Segmental ostectomy of both fibulae (7 mm) was performed, and the defect area was then grafted with xenogenic bone with different bisphosphonate concentrations. Alternatively, the left and right fibulae were treated with absorbable collagen sponges or xenogenic bone with application of rhBMP-2. After 4 or 8 weeks, animals were sacrificed, and radiographic, histological, histomorphometrical, and immunohistochemical analyses were performed. The results showed that higher concentrations of bisphosphonate were associated with greater bone formation than lower concentrations of bisphosphonate. Moreover, rhBMP-2 promoted bone formation, regardless of the carrier; fibula grafted with collagen sponges or xenogenic bone exhibited continuity between the graft material and defect area. Additionally, the newly formed cortical layer was similar in appearance to the original fibula cortex, particularly after 8 weeks. A comparison of high-concentration bisphosphonate and rhBMP-2 revealed that these treatments had similar osteoinductive abilities, with slightly less bone formation observed for bisphosphonate. In conclusion, the locally application of bisphosphonate promoted new bone formation, particularly when used at high concentrations. Absorbable collagen sponges were advantageous in

that there was no remaining graft material and that the bone was remodeled to resemble the existing fibula. In order to use these materials as a substitute for original bone, further studies regarding stability and mechanical strength are needed.

Key words : Bisphosphonate, rhBMP-2, Bone formation, Xenogenic bone graft, Absorbable collagen sponge

Effects of locally administered bisphosphonate and rhBMP-2 on bone regeneration in the rat fibula

Eun-Jung Kwak

Department of Dentistry

The Graduate School, Yonsei University

(Directed by Professor Hyung Jun Kim, DDS, PhD)

1. Introduction

Bone grafting using autogenous, xenogenic, and allogenic bone is usually performed to reconstruct bone defects after trauma or operation in oral and maxillofacial surgery. Autogenic bone grafting is typically the recommended treatment. However, in cases of large primary defects or limited donor sites, xenogenic or allogenic bone grafting is required. Unfortunately, xenografting and allografting are limited because they only function in osteoconduction. Accordingly, most studies of bone grafting have examined both the graft material and the use of bone morphogenetic factors. For example, an early study in 1965 reported the osteogenic effects of recombinant human bone morphogenetic protein-2 (rhBMP-2) (Urist, 1965). Subsequently, many researchers have aimed to identify, isolate, and synthesize bone morphogenetic proteins (BMPs). More than seven

types of BMPs, belonging to the transforming growth factor (TGF) superfamily, have been identified (Schilephake, 2002).

rhBMP-2 is known to induce new bone formation during the bone healing period, and the osteoinductive effects of rhBMP-2 have been studied extensively. A recent study examined new bone formation using rhBMP-2 with bone graft materials in maxillary sinus floor augmentation (Kim et al., 2015). Additionally, a serial study comparing an absorbable collagen sponge with saline and rhBMP-2 confirmed the inducible ability of rhBMP-2 (Park, 2010). An absorbable collagen sponge with rhBMP-2 was found to be more effective than xenogenic bone graft material with saline in segmental bone defects in a previous study (Baek, 2013). However, no studies have evaluated effective carriers for rhBMP-2.

Local administration of bisphosphonate has been shown to promote bone formation (Kwon, 2011); however, the optimal concentration of bisphosphonate has not been determined. Therefore, in this study, we compared xenogenic (porcine) bone and absorbable collagen sponges to identify an appropriate rhBMP-2 carrier and evaluated the bone healing effects of locally administration of bisphosphonate in critical size segmental bone defects in the fibulae of Sprague-Dawley rats.

2. Materials and Methods

2.1. Animals

Thirty-two male Sprague-Dawley rats (8 weeks old; weighing between 250 and 300 g; Orient Bio, Korea) were used in this study. The rats were housed individually in standard rat cages and maintained under constant temperature and humidity, with a 12-h light/dark schedule. Purified drinking water and a pellet diet were supplied. Animals were allowed to acclimate for 1 week prior to use in experiments. All animal protocols were approved by the Institutional Animal Use and Care Committee of the Department of Laboratory Animal Resources, Yonsei Biomedical Research Institute, Yonsei University College of Medicine, Korea.

2.2. Experimental design

2.2.1. Experiment 1

Segmental ostectomy (7 mm) was performed in both fibulae of 16 rats. The left fibulae were grafted with xenogenic bone (CollaOss; Bioland, Korea) dipped in low-concentration alendronate (1 mM; Cayman Chemical, USA), whereas the right fibulae were grafted with xenogenic bone dipped in high-concentration alendronate (10 mM).

The concentrations of alendronate used in this study were based on a previous study (Kim et al., 2015). We did not use a control group because a previous study (Baek, 2013) reported the same experimental model with xenogenic bone grafting alone in segmental fibula defects (Table 1, Figure 1). Additionally, the size of the defect (7 mm) was chosen based on a previous study (Park, 2010) in which grafting with an absorbable collagen sponge alone after segmental ostectomy of fibula did not result in new bone formation. Similarly, in a segmental bone defect model in rat fibulae, new bone did not form in 6-mm fibula defects by 12 weeks postsurgery (Hollinger and Kleinschmidt, 1990).

Table 1. Study design of experiment 1.

		Group(n)	Graft
Experimental Group 1	Lt. Fibula	4wks(8)	Xenogenic bone (CollaOss®) Alendronate 1mM (32.5μg)
		8wks(8)	Xenogenic bone (CollaOss®) Alendronate 1mM (32.5μg)
	Rt. Fibula	4wks(8)	Xenogenic bone (CollaOss®) Alendronate 10mM (325μg)
		8wks(8)	Xenogenic bone (CollaOss®) Alendronate 10 mM (325μg)

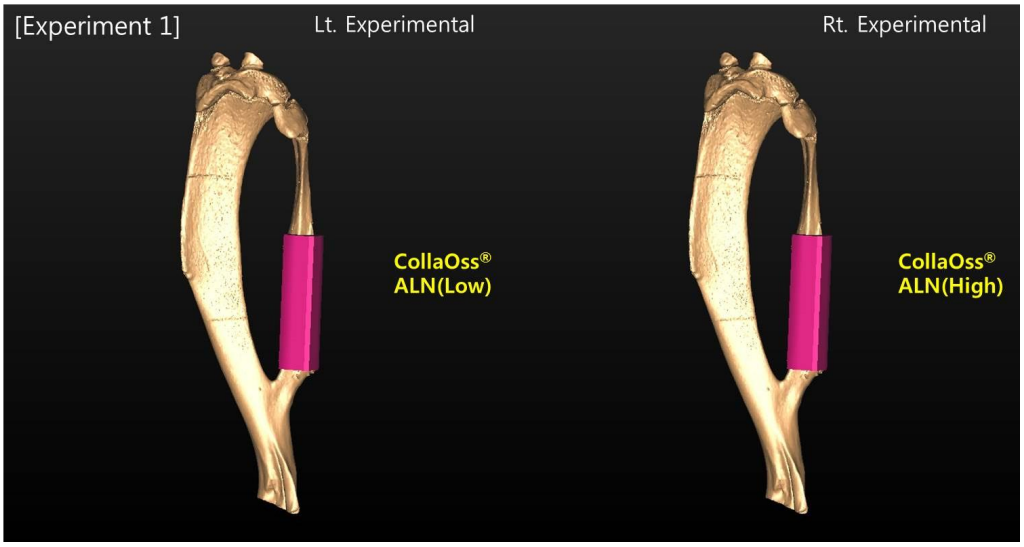

Figure 1. Schematic study design of experiment 1.

2.2.2. Experiment 2

Segmental ostectomy (7 mm) was performed in both fibulae of 16 rats. Left fibulae were grafted with absorbable collagen sponges (Rapiderm Pad; Dalim Tissen, Korea) containing 10 μg rhBMP-2 (CowellBMP; Cowell Medi, Korea), whereas right fibulae were grafted with xenogenic bone (CollaOss) containing 10 μg rhBMP-2. We did not use a control group because a previous study (Park, 2010) reported the same experimental model with absorbable collagen sponge grafts alone in segmental fibula (Table 2, Figure 2).

Table 2. Study design of experiment 2.

		Group(n)	Graft
Experimental Group 2	Lt. Fibula	4wks(8)	Absorbable collagen sponge (Rapiderm Pad®) rhBMP-2 10μg
		8wks(8)	Absorbable collagen sponge (Rapiderm Pad®) rhBMP-2 10μg
	Rt. Fibula	4wks(8)	Xenogenic bone (CollaOss®) rhBMP-2 10μg
		8wks(8)	Xenogenic bone (CollaOss®) rhBMP-2 10μg

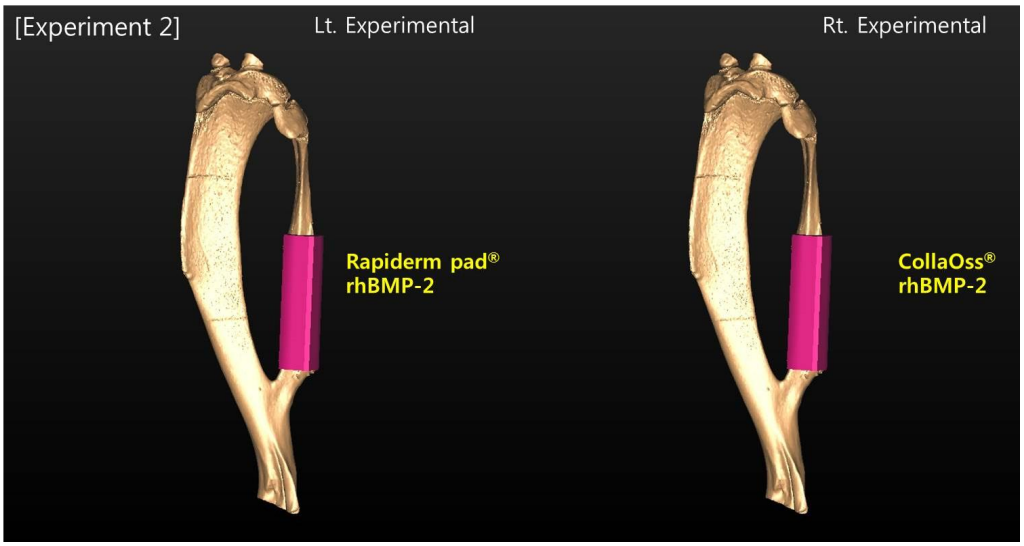

Figure 2. Schematic study design of experiment 2.

2.3. Surgical procedure

Animals were anesthetized using isoflurane (Forane; JW, Korea; Figure 3). The surgical site was shaved and cleaned with 10% povidone-iodine (Betadine; Korea Pharma Co. Ltd., Korea), and rats were placed under sterile drapes. A 1.5-cm skin and muscular incision was performed above the fibula, and about 1 cm of fibula was exposed. A 7-mm area was measured using vernier calipers, and segmental ostectomy was performed using dean scissors. Graft materials measuring 4 × 4 × 8 mm were used (Figure 4).

In experiment 1, bisphosphonate solution was prepared by dissolving alendronate in saline and filtering through a 0.2-μm Millipore filter (Merck Millipore Ltd., Cork, Ireland). In experiment 2, the rhBMP-2 was rehydrated with saline and prepared at a concentration of 0.1 mg/mL. The graft material was treated with 0.1 mL of this solution (10 μg) using a micropipette.

The incision was closed layer by layer with absorbable 4-0 Vicryl sutures (Johnson & Johnson, Korea) for muscle and subcutaneous tissue and nylon 5-0 Ethilon sutures (Johnson & Johnson) for skin. The graft material was stabilized by suturing of the muscle cuff (Figure 4).

To prevent postoperative infection and reduce pain, antibiotics (0.05 mL/day; Baytril; Bayer, Korea) were administered by intramuscular injection, and meloxicam powder (0.75 mg/day; Mobic; Boehringer Ingelheim) was administered via drinking water.

The experimental rats were sacrificed by CO_2 inhalation randomly at 4 or 8 weeks after surgery for both groups. The tibiae and fibulae were harvested and evaluated clinically, radiographically, and histologically.

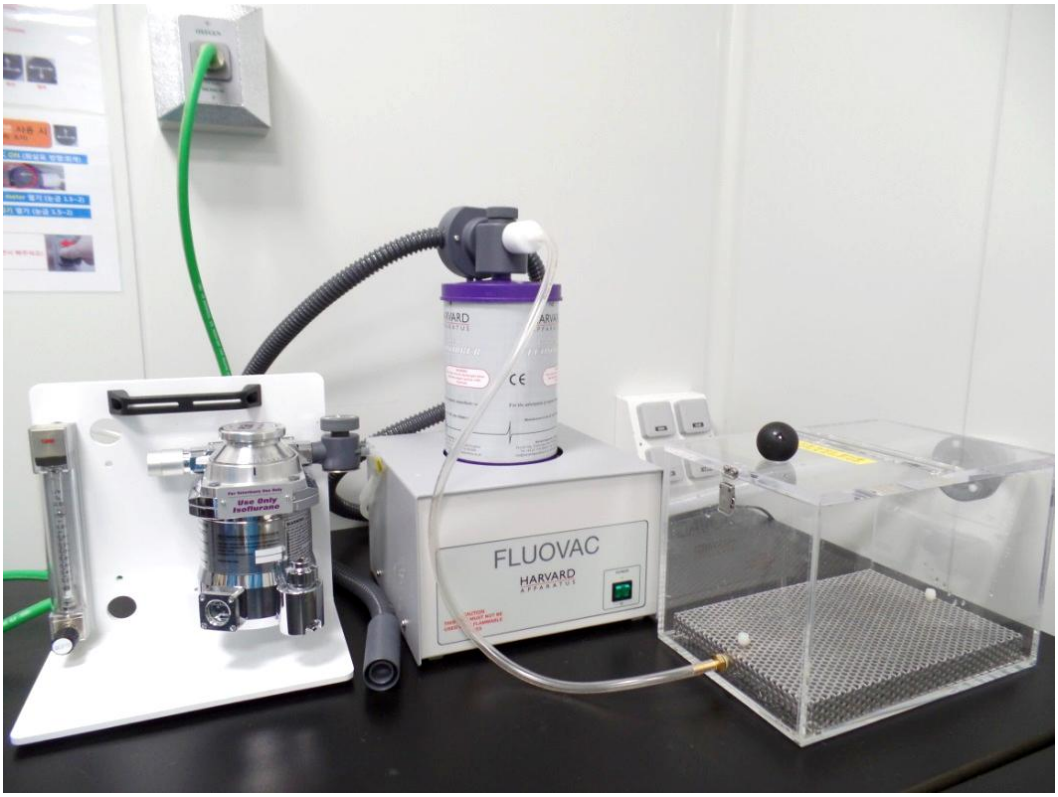

Figure 3. Inhalation anesthesia instruments.

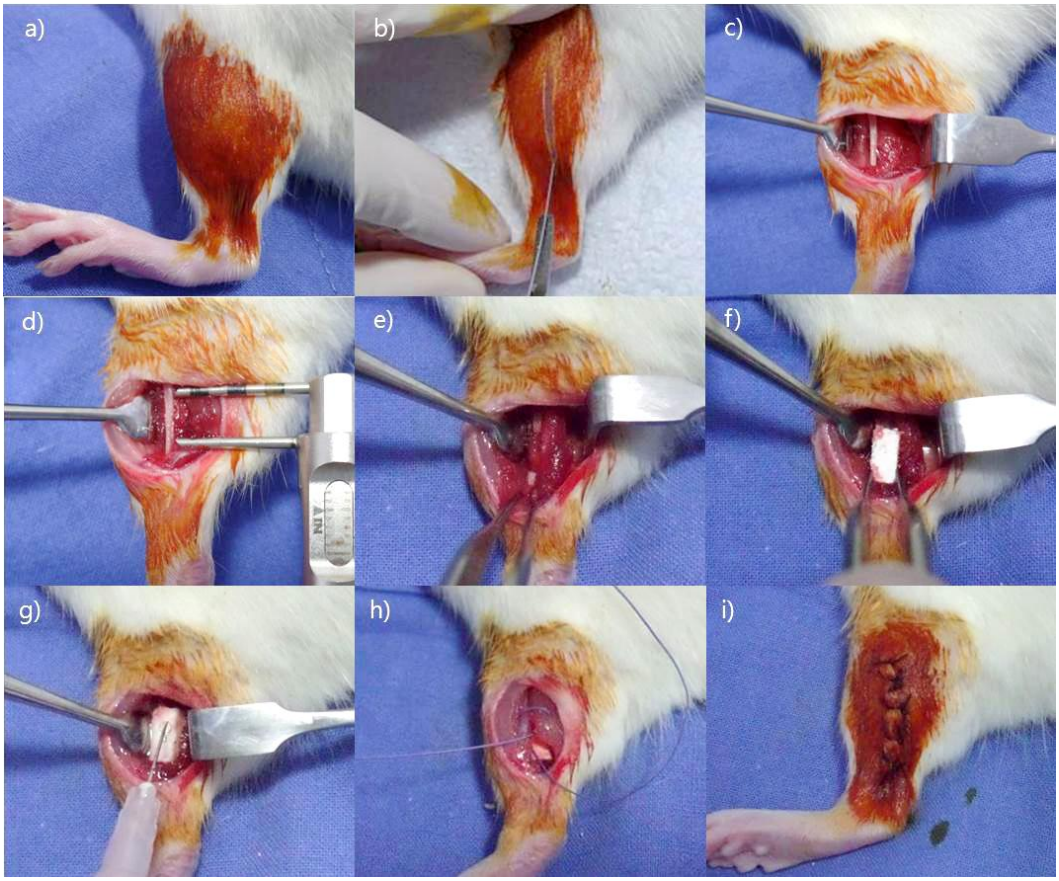

Figure 4. Procedure of alendronate or rhBMP-2 loaded CollaOss® or Rapiderm pad® graft. a) Operation field cleaned by iodine; b) 1.5cm skin incision; c) Exposed fibula; d) 7mm was measured with caliper; e) 7mm sized segmental defect on fibula; f) Graft of prefabricated CollaOss® or Rapiderm pad®; g) alendronate or rhBMP-2 is applicated on graft material; h) Layer by layer suturing; i) Postoperative dressing.

2.4. Assessment methods

2.4.1. Plain radiographic evaluation

Fibulae and tibiae specimens were placed between digital film and an x-ray tube (voltage, 60 kV; current, 70 mA; exposure, 0.08 s). Each digital image was assessed.

2.4.2. Micro-computed tomography (micro-CT)

The specimens were evaluated by micro-CT using a SkyScan 1173 scanner (SkyScan; Bruker-CT, Kontich, Belgium) with the source voltage and current set to 130 kV and 60 μA, respectively, and a rotation step size of 0.3° over a trajectory of 360°. Images were acquired with an image pixel size of 22.02 μm, a 1.0-mm aluminum filter to optimize contrast, a frame averaging of 4 to reduce noise, and an exposure time of 500 ms. Three-dimensional (3D) image reconstruction was then performed using Nrecon software (SkyScan) with a beam hardening correction set to 40%. Images had a pixel size of 22.02 μm and an angular step of 0.3°. The densities of the original fibula and graft area were assessed in Hounsfield units (HU) with Dataviewer software (SkyScan, Version 1.4.3). The 3D image analysis program CTAn (SkyScan) was used to select the total regeneration area as the region of interest (ROI). All ROIs were then divided by as follows: total bone (TB; 50–255 HU), connective tissue (CT, 50–85 HU), new bone (NB, 86–130 HU), and remaining bone material (BM, 131–255 HU). The volumes between thresholds were evaluated.

2.4.3. Histology and histomorphometry

All harvested specimens were labeled and fixed in 10% formalin just after sacrifice. Samples were then decalcified with 10% ethylenediaminetetraacetic acid (EDTA; Chelator Cal, BBC, Mount Vernon, WA, USA) buffer (pH 7.4) for 4 weeks. The EDTA was changed every 2 or 3 days and stored at 4°C until the specimens were adequately decalcified. Samples were then dehydrated in increasing concentrations of alcohol (70%, 95%, and 100%), embedded in paraffin containing dimethylsulfoxide (Paraplast Plus; Leica Biosystems Richmond, Inc., Richmond, IL, USA) using peel-away embedding molds (37 × 24 × 5 mm), and incubated overnight at 4°C. The serial sections (5 μm) were created along the longitudinal axis of the fibula. The selected sections were mounted on slides coated with poly-L-lysine (Superfrost-20; Matsunami Glass Ind, Kishiwada Osaka, Japan), deparaffinized in xylene, rehydrated in four sequential ethanol baths (from 99.9% to 70% ethanol), and stained with hematoxylin and eosin (H&E) and Masson-Trichrome (M-T) for histological analysis.

Histological images were examined at ×10, ×40, ×100, and ×200 magnification using Caseviewer (3DHISTECH Ltd., Budapest, Hungary). Specific areas including the segmental resection margin and graft were selected (Figure 5). A portion of remaining bone material, new bone, and adipose tissue within the total area were compared in selected areas. Images were analyzed using Adobe Photoshop CS4 (Adobe Systems, Inc., San Jose, CA, USA; Figure 6).

The thickness of the cortical layer was measured using the Caseviewer program (Figure 7).

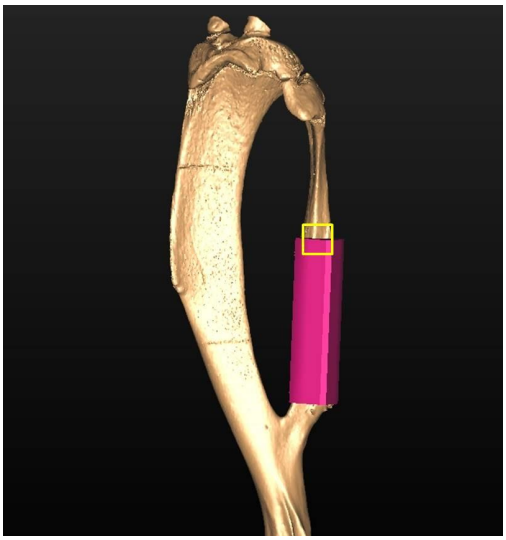

Figure 5. The selected area of resection margin and graft analyzed in histomorphometry.

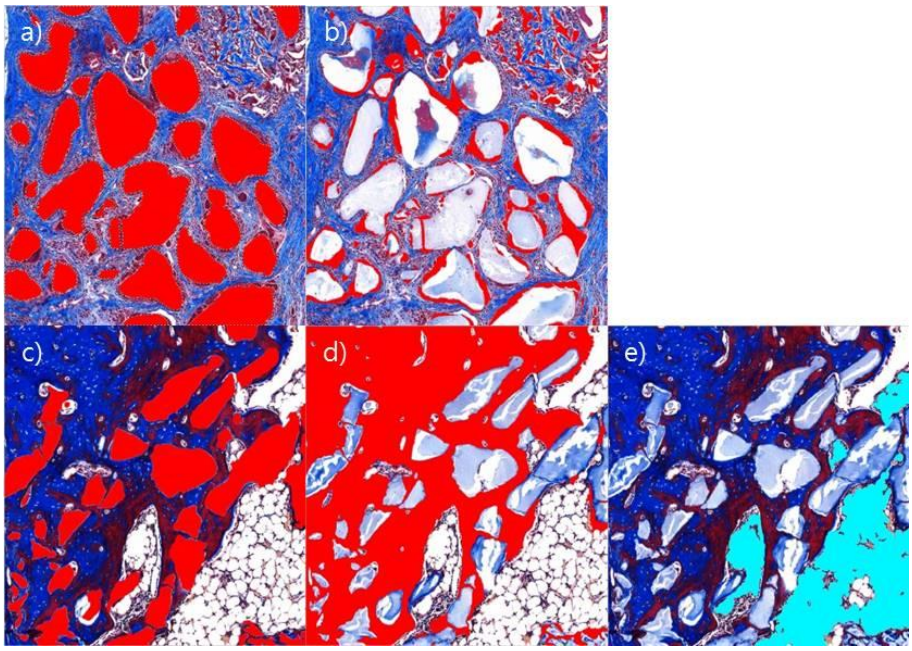

Figure 6. Measurement of bone material, newly formed bone, adipose tissue by Adobe Photoshop CS4. Area of remaining bone material, newly formed bone and adipose tissue

were calculated drawing the outlines and coloring each portion. a), b) experiment 1; c), d), e) experiment 2; a) remaining bone material; b) newly formed bone; c) remaining bone material; d) newly formed bone; e) adipose tissue.

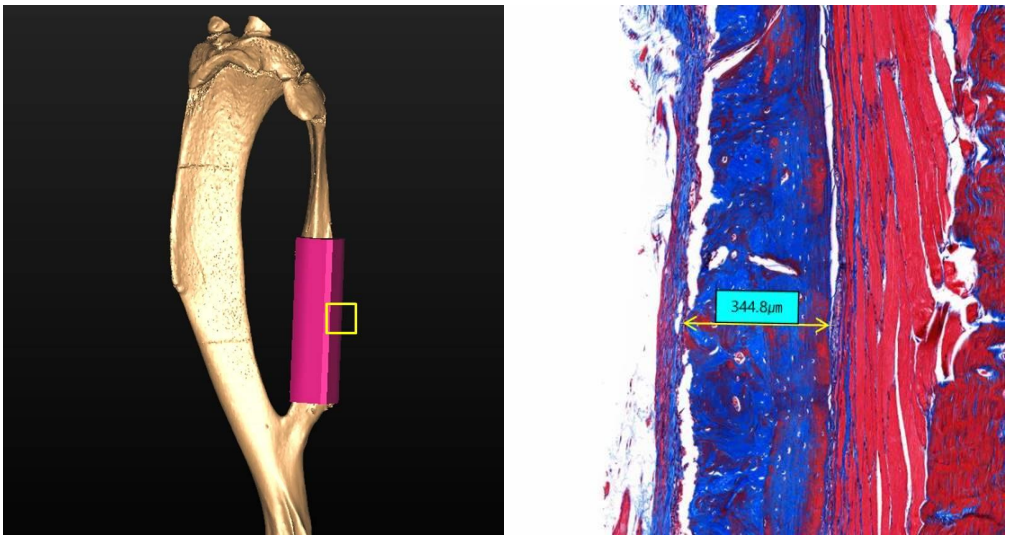

Figure 7. The selection of area and measuring thickness of cortical layer.

2.4.4. Immunohistochemistry

The sections were used to identify the expression of BMP2 and OPG using appropriate antibodies (ab6285 for anti-BMP2 antibodies; ab73400 for anti-OPG antibodies; Abcam, UK) in the grafted area. Antigen retrieval for BMP2 and OPG was performed by incubation with 10mM sodium citrate buffer (pH 6.0) for 30 min at 95°C. The sections were then incubated with the primary antibody at a 1:100 dilution for 2 h at 37°C. Detection was performed using 3,3'-diaminobenzidine (DAB; Abcam), and hematoxylin was used as background staining for 20–120 s to facilitate visualization.

2.5. Statistical analysis

Statistical analysis was performed with nonparametric Mann-Whitney tests using SPSS 24.0. Differences with *p* values of less than 0.05 were considered statistically significant.

3. Results

3.1. Gross examination

3.1.1. Experiment 1

At 4 weeks after grafting, continuity was observed between the bone defect and graft material; however, some of the bone material was separated from the graft material in both the left and right fibulae. There were no significant differences between the low and high concentrations of alendronate at this time point.

At 8 weeks, continuity between the resection margin and graft area was examined; however, some of the materials at the edge of the samples were separated from the main bone material. However, similar to the findings at 4 weeks, there were no significant differences between the low and high concentrations of alendronate at 8 weeks.

3.1.2. Experiment 2

At 4 weeks, the graft material and defect bone site were connected. The right fibula, which was grafted with xenogenic bone, was more dense and compact than the left fibula, which was grafted using absorbable collagen sponges as a carrier for rhBMP-2.

At 8 weeks, continuity between the graft material and defect area was observed. Moreover, the appearance of the right fibula was more solid than that of the left fibula. Finally, a more solid connection was observed for the left fibula and graft materials at 8 weeks than at 4 weeks.

3.2. Radiographic evaluation

3.2.1. Experiment 1

At 4 weeks, plain X-ray results were similar to the findings of gross examination. Remaining bone graft material was observed, with some specimens showing disconnection from the bone. No significant differences were observed between left and right fibulae; however, the right fibula exhibited a more dense and continuous structure than the left fibula (Figure 8).

At 8 weeks, less separated bone graft material was observed compared with that at 4 weeks. Additionally, the size of the graft material was smaller than that at 4 weeks because of resorption. Similar to the results at 4 weeks, a more compact appearance was observed for the samples treated with high alendronate compared with that treated with low alendronate (Figure 9).

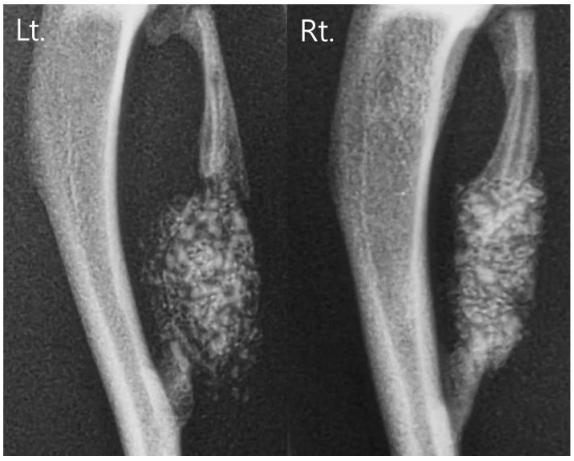

Figure 8. Radiographic findings (Plain x-ray) of 4-week experimental group 1 on left (xenogenic bone with low concentrate bisphosphonate) and right (xenogenic bone with high concentrate bisphosphonate) side.

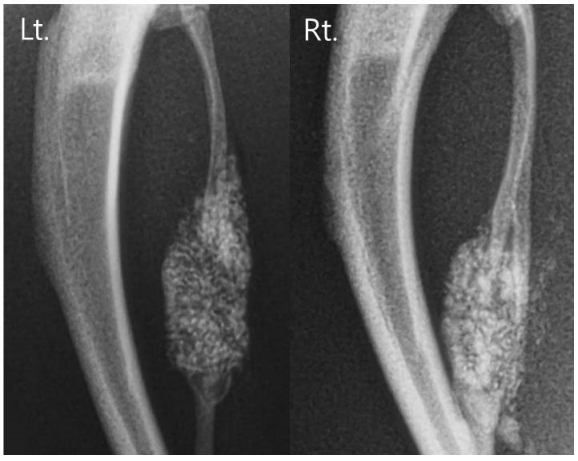

Figure 9. Radiographic findings (Plain x-ray) of 8-week experimental group 1 on left (xenogenic bone with low concentrate bisphosphonate) and right (xenogenic bone with high concentrate bisphosphonate) side.

3.2.2. Experiment 2

At 4 weeks after grafting, the continuity between the grafted area and original fibula exhibited prominent continuity. However, for the left fibula, grafted with the absorbable collagen sponge, some noncontinuous portions were observed relative to that observed in the right fibula. Additionally, a considerable amount of remaining bone graft material was observed for the right fibula, which was grafted with xenogenic bone (Figure 10).

At 8 weeks, the connection between the fibula defect and bone graft was much more smooth and solid than that observed at 4 weeks for both the left and right fibulae. Only a small portion of bone graft material remained for the right fibula (Figure 11).

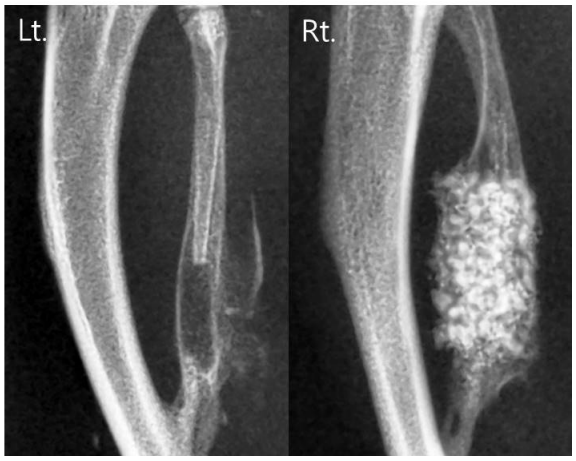

Figure 10. Radiographic findings (Plain x-ray) of 4-week experimental group 2 on left (absorbable collagen sponge with rhBMP-2) and right (xenogenic bone with rhBMP-2) side.

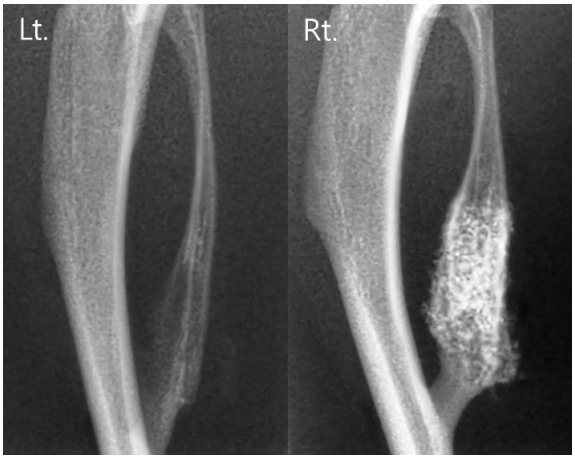

Figure 11. Radiographic findings(Plain x-ray) of 8-week experimental group 2 on left (absorbable collagen sponge with rhBMP-2) and right (xenogenic bone with rhBMP-2) side.

3.3. Micro-CT evaluation

3.3.1. Experiment 1

At 4 weeks, examination of the left fibula by micro-CT showed similar results as those observed by gross examination and radiographic evaluation. Most of the grafted area showed higher density than the bone marrow of the tibia. Additionally, some graft material resembled the cortical bone of the tibia (Figure 12). The average volume of TB relative to the total volume of the ROI was 70.37%, and the average volumes of CT, NB, and BM relative to that of TB were 57.84%, 25.82%, and 16.34%, respectively (Figure 13).

Similarly, for the right fibula at 4 weeks, the micro-CT results were consistent with the clinical and radiographic examinations. The remaining bone material exhibited a denser appearance in the right fibula than in the left fibula (Figure 14). The average volume of TB relative to the total volume of the ROI was 61.71%. The average volumes of CT, NB, and BM relative to that of TB were 56.88%, 29.60%, and 13.52%, respectively. The proportion of newly formed bone was slightly higher in the right fibula, treated with a higher concentration of alendronate, and remaining bone material was higher in the left fibula, treated with a lower concentration of alendronate (Figure 13).

At 8 weeks, in the left fibula, the remaining bone size was reduced compared with that at 4 weeks (Figure 15). The average volume of TB relative to the total volume of the ROI was 64.99%. The average volumes of CT, NB, and BM relative to that of TB were 48.81%, 33.46%, and 17.73%, respectively. The rate of new bone formation increased by

7.64%, and connective tissue decreased by 9.03% (Figure 13). For the right fibula at 8 weeks, micro-CT data showed that the defect area was more dense than the original marrow bone (Figure 16). The average volume of TB relative to the total volume of the ROI was 57.79%. The average volumes of CT, NB, and BM relative to that of TB were 40.31%, 39.97%, and 19.72%, respectively. The rate of new bone formation increased by 10.37%, and connective tissue decreased by 16.57% (Figure 13).

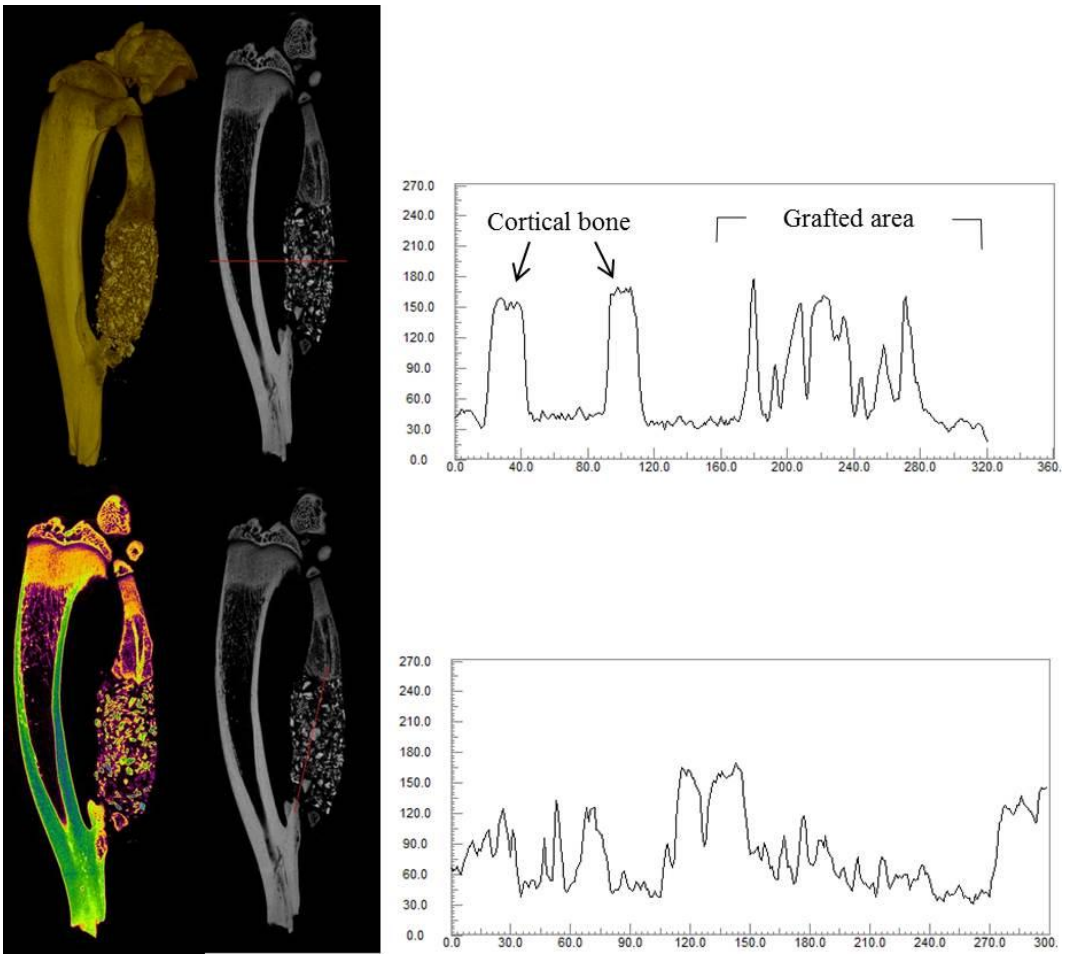

Figure 12. 3-dimensional reconstruction image, Long axis CT view of 4-week left fibula in experiment 1. Bone density was measured along the red line. In graphs, x-axis means length (pixel), and y-axis means bone density (Hounsfield unit).

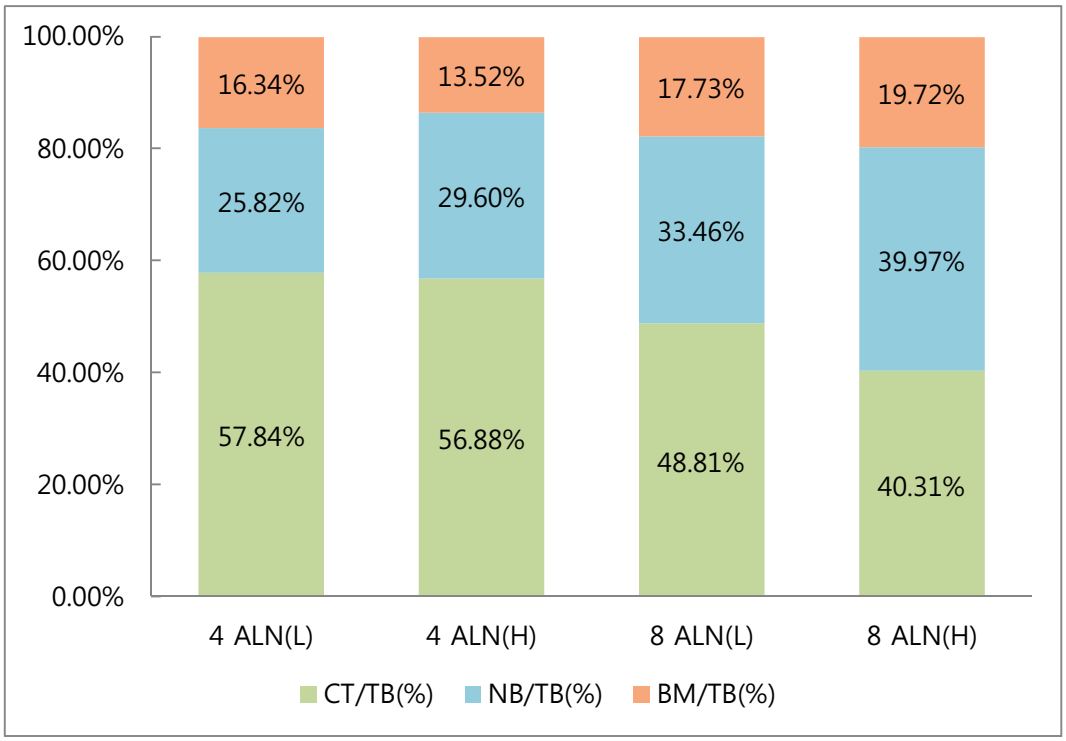

Figure 13. The rate of CT, NB, BM of experimental group 1. CT, connective tissue; NB, new bone; BM, bone material; TB, total bone; 4 ALN(L), low alendronate group of 4 weeks; 4 ALN(H), high alendronate group of 4 weeks; 8 ALN(L), low alendronate group of 8 weeks; 8 ALN(H), high alendronate group of 8 weeks.

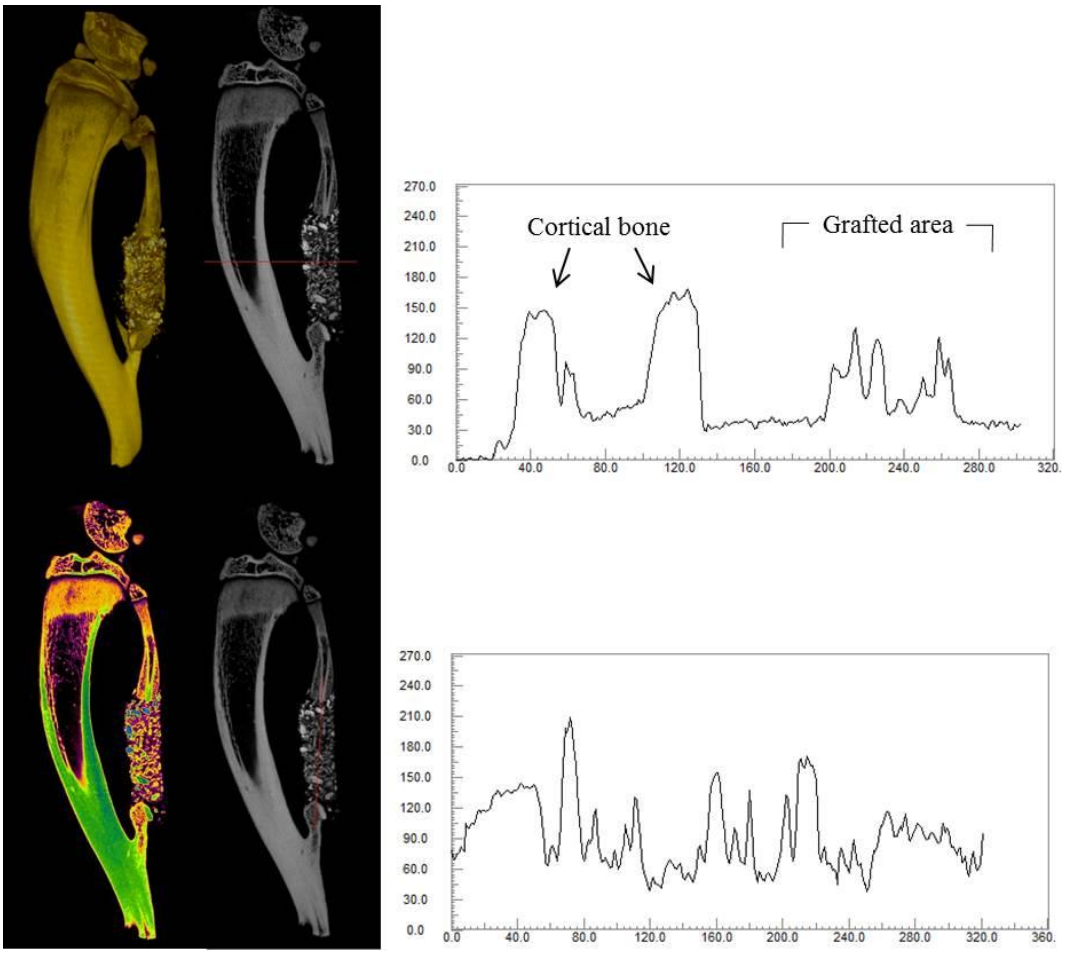

Figure 14. 3-dimensional reconstruction image, Long axis CT view of 4-week right fibula in experiment 1. Bone density was measured along the red line. In graphs, x-axis means length (pixel), and y-axis means bone density (Hounsfield unit).

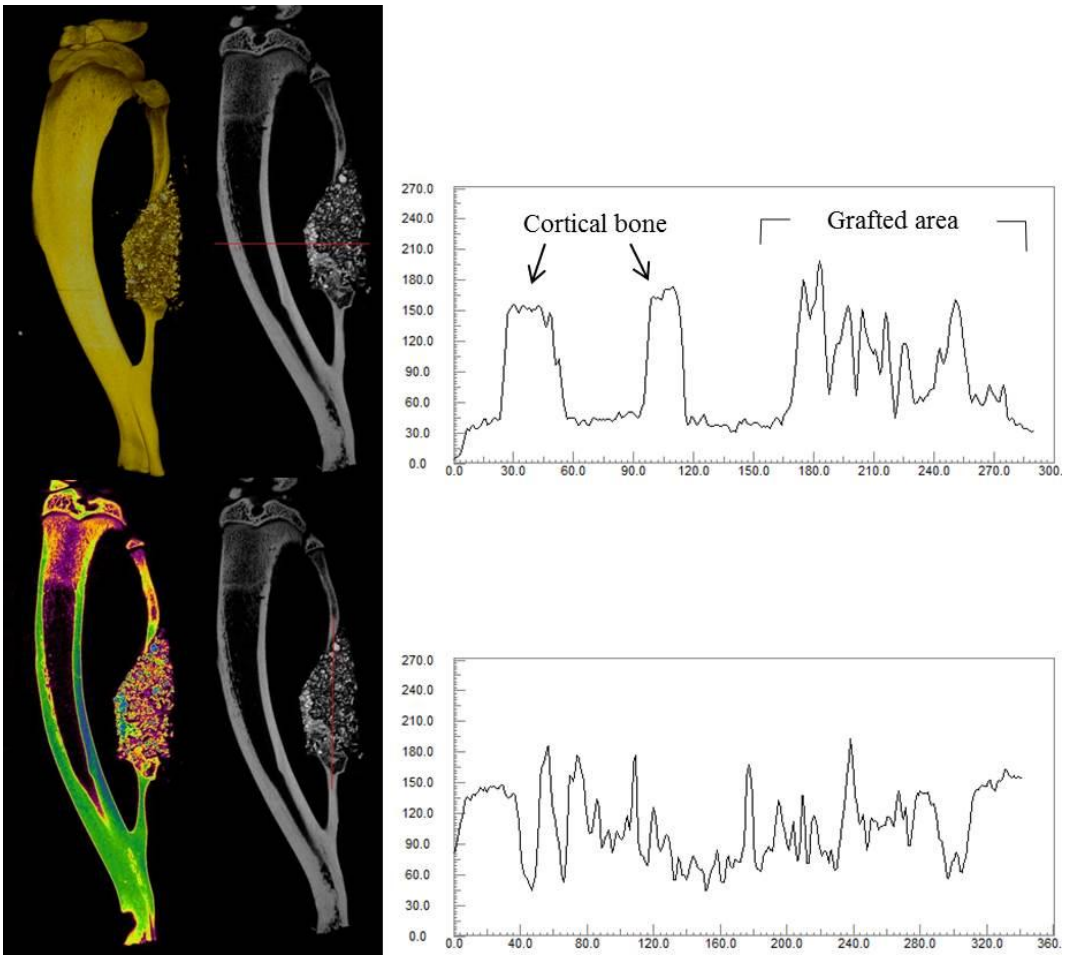

Figure 15. 3-dimensional reconstruction image, Long axis CT view of 8-week left fibula in experiment 1. Bone density was measured along the red line. In graphs, x-axis means length (pixel), and y-axis means bone density (Hounsfield unit).

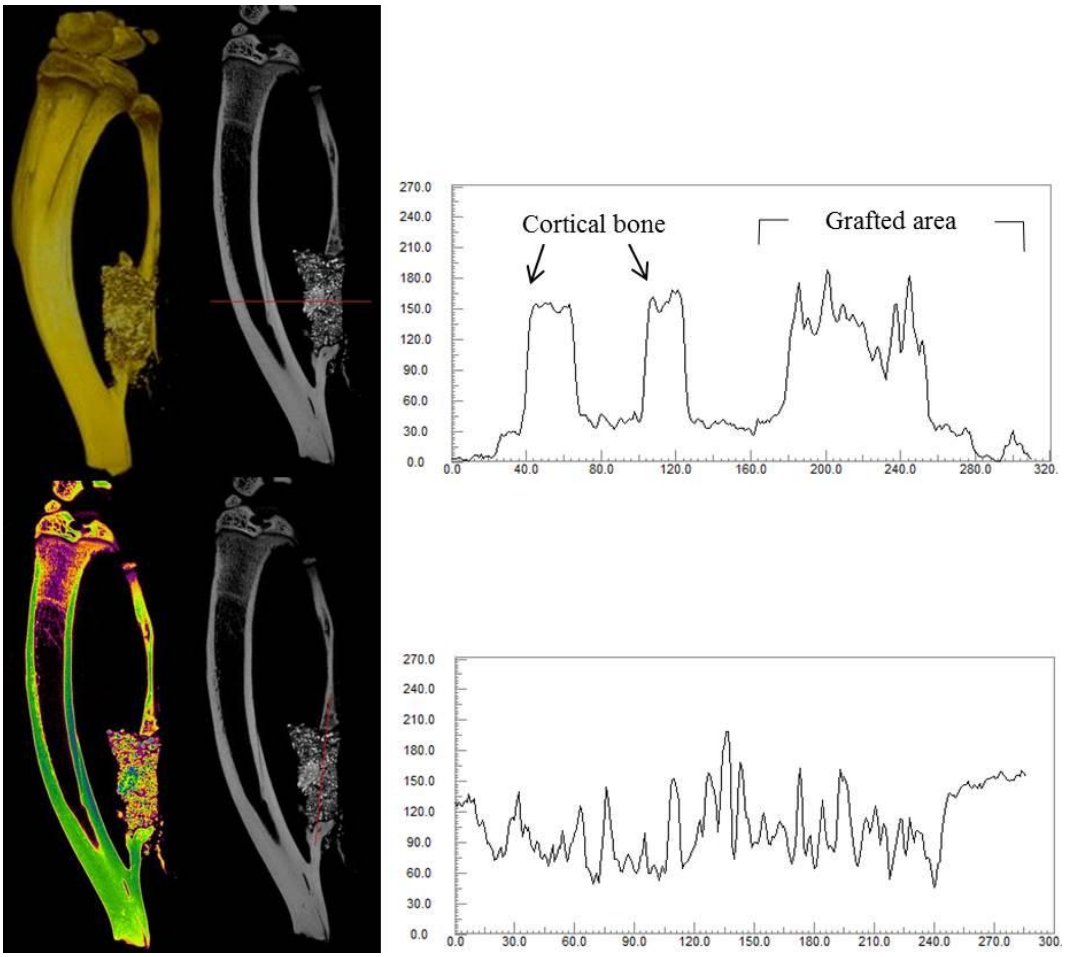

Figure 16. 3-dimensional reconstruction image, Long axis CT view of 8-week right fibula in experiment 1. Bone density was measured along the red line. In graphs, x-axis means length (pixel), and y-axis means bone density (Hounsfield unit).

3.3.2. Experiment 2

In the left fibula at 4 weeks, continuity with neighboring resected margins was observed in gross and plain radiographic evaluations (Figure 17). The average volume of TB relative to the total volume of the ROI was 27.08%. The average volumes of CT and NB relative to that of TB were 65.63% and 32.40%, respectively. The rate of new bone formation was the lowest of all groups at 4 weeks (Figure 18); indeed, the amounts of connective tissue and new bone were 19.59 and 9.33 mm^3, respectively, for the left fibula and 39.61 and 30.25 mm^3, respectively, for the right fibula.

For the right fibula at 4 weeks, there were no differences among gross observations and plain radiographic findings. The continuous appearance of the graft material and end of the fibula was more obvious in the rhBMP-2 group than in the alendronate group (Figure 19). The average volume of TB relative to the total volume of the ROI was 79.72%. The average volumes of CT, NB, and BM relative to that of TB were 44.91%, 33.91%, and 21.17%, respectively (Figure 18).

At 8 weeks, the regenerated bone in the left fibula was similar to that of the existing fibula and connected naturally. The density of the newly formed cortical layer was increased relative to that at 4 weeks. The medial side was thicker and denser than the lateral side (Figure 20). The average volume of TB relative to the total volume of the ROI was 21.60%. The average volumes of CT and NB relative to that of TB were 43.68% and 46.29%, respectively. Thus, the rate of new bone increased by 13.89%, and connective tissues decreased by 21.95% compared with those at 4 weeks (Figure 18). Numerical

values for connective tissue and new bone were 10.34 and 11.01 mm^3, respectively, for the left fibula and 28.79 and 26.82 mm^3, respectively, for the right fibula.

For the right fibula at 8 weeks, continuity between the bone graft material and the segmental resection margin was more solid than that in the other group. The threshold value in the outer layer of the grafted area was similar to that of the cortical bone in the tibia (Figure 21). The average volume of TB relative to the total volume of the ROI was 75.95%. The average volumes of CT, NB, and BM relative to that of TB were 34.67%, 32.18%, and 33.15%, respectively. The rates of newly formed bone were similar, and connective tissue decreased by 10.24% (Figure 18).

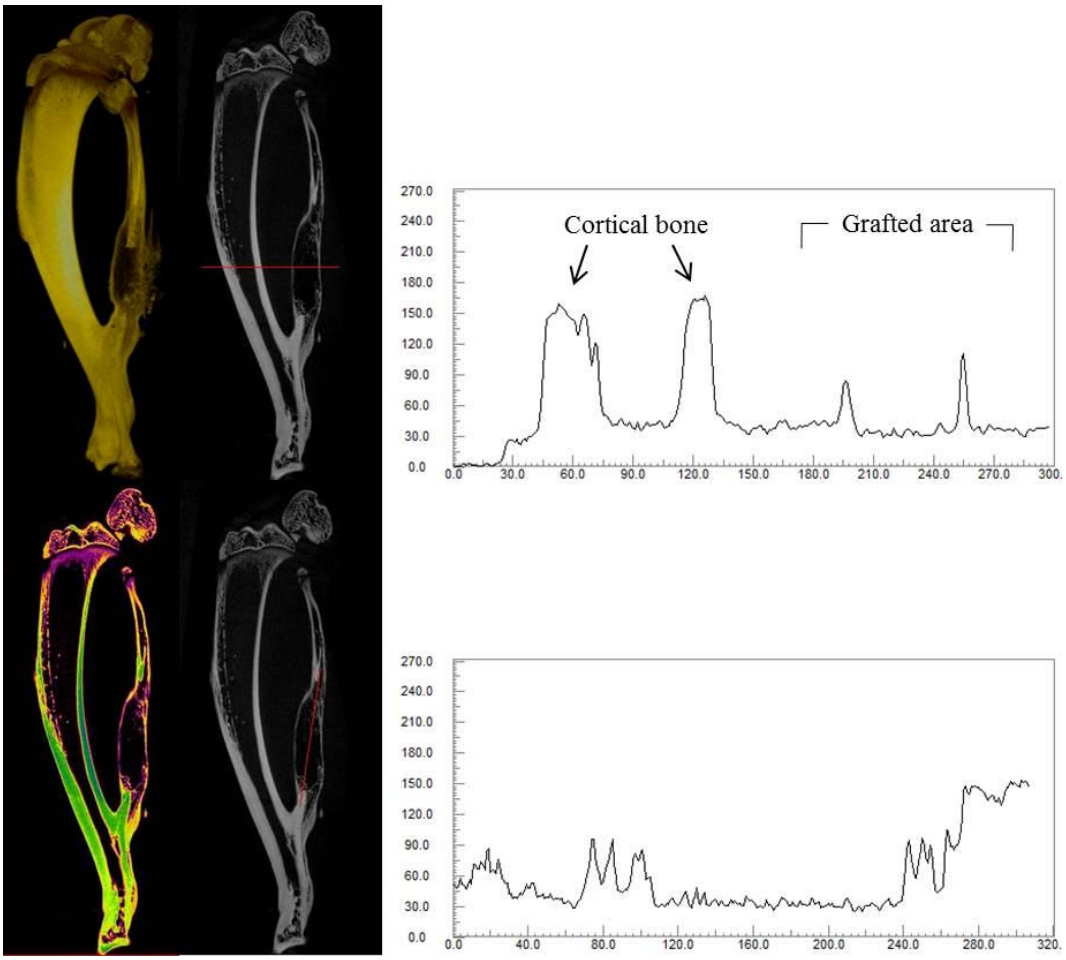

Figure 17. 3-dimensional reconstruction image, Long axis CT view of 4-week left fibula in experiment 2. Bone density was measured along the red line. In graphs, x-axis means length (pixel), and y-axis means bone density (Hounsfield unit).

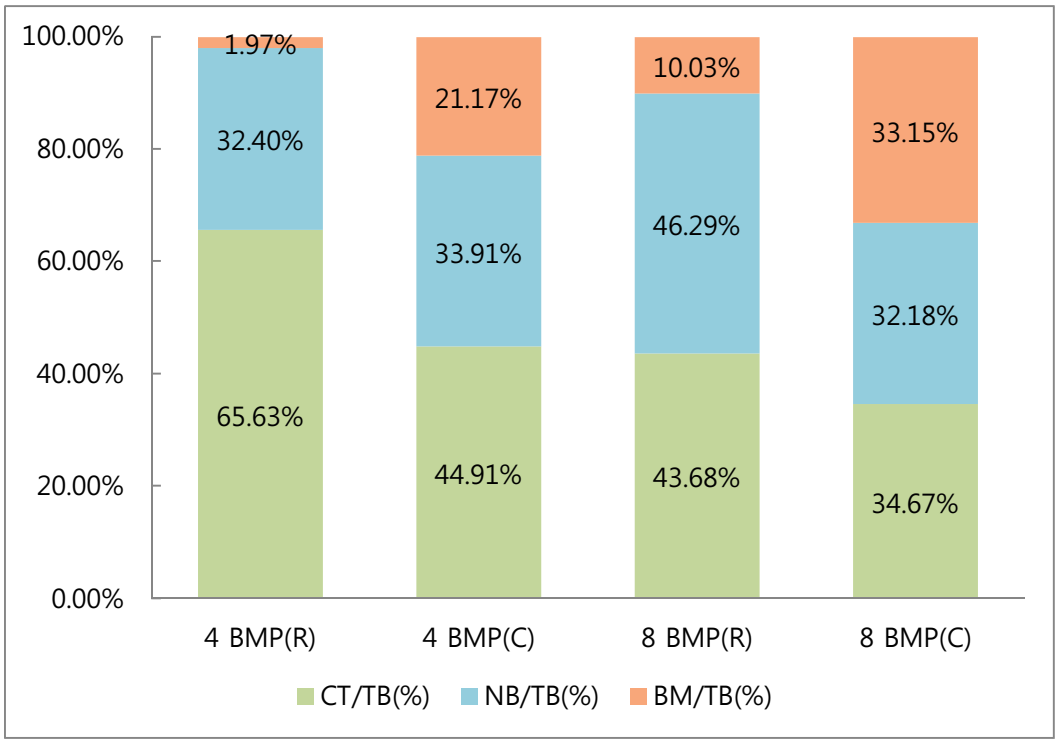

Figure 18. The rate of CT, NB, BM of experimental group 2. CT, connective tissue; NB, new bone; BM, bone material; TB, total bone; 4 BMP(R), rhBMP-2 group with Rapiderm pad® of 4 weeks; 4 BMP(C), rhBMP-2 group with CollaOss® of 4 weeks; 8 BMP(R), rhBMP-2 group with Rapiderm pad® of 8 weeks; 8 BMP(C), rhBMP-2 group with CollaOss® of 8 weeks.

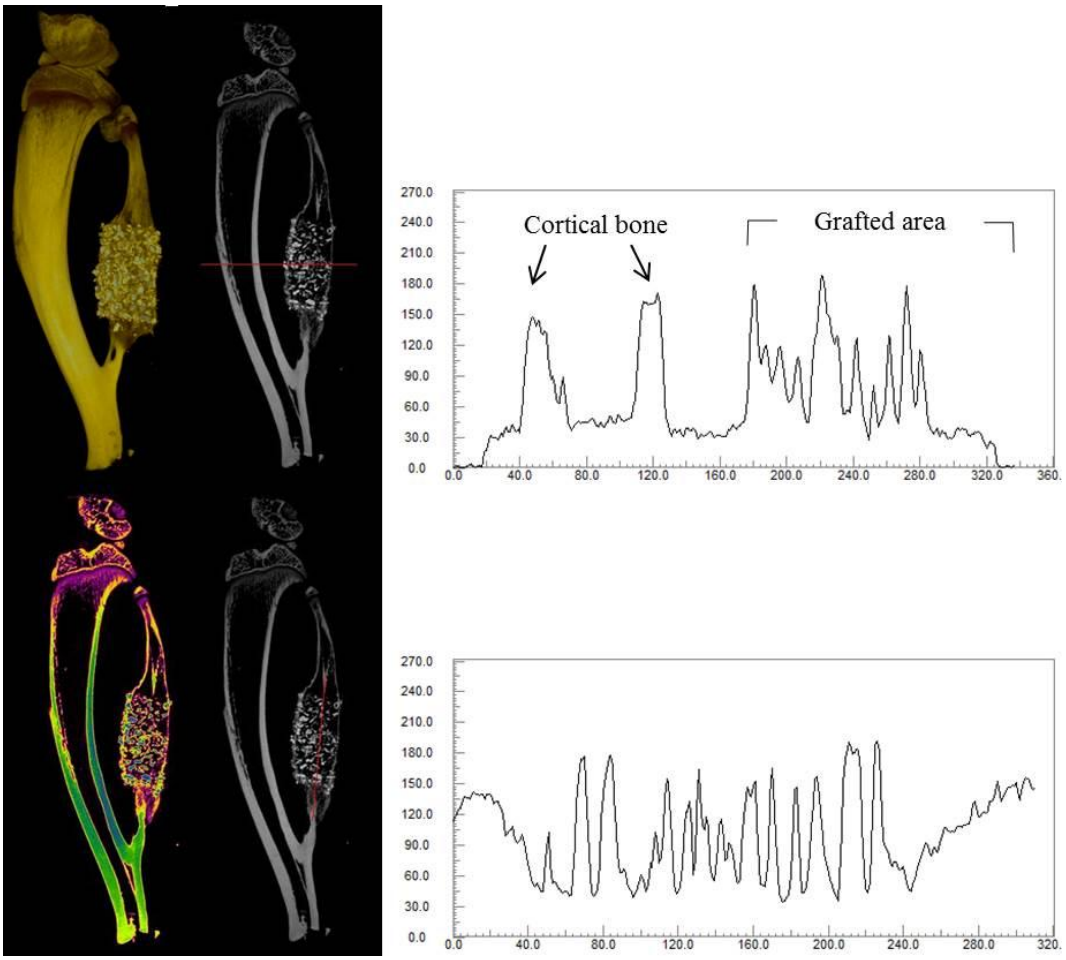

Figure 19. 3-dimensional reconstruction image, Long axis CT view of 4-week right fibula in experiment 2. Bone density was measured along the red line. In graphs, x-axis means length (pixel), and y-axis means bone density (Hounsfield unit).

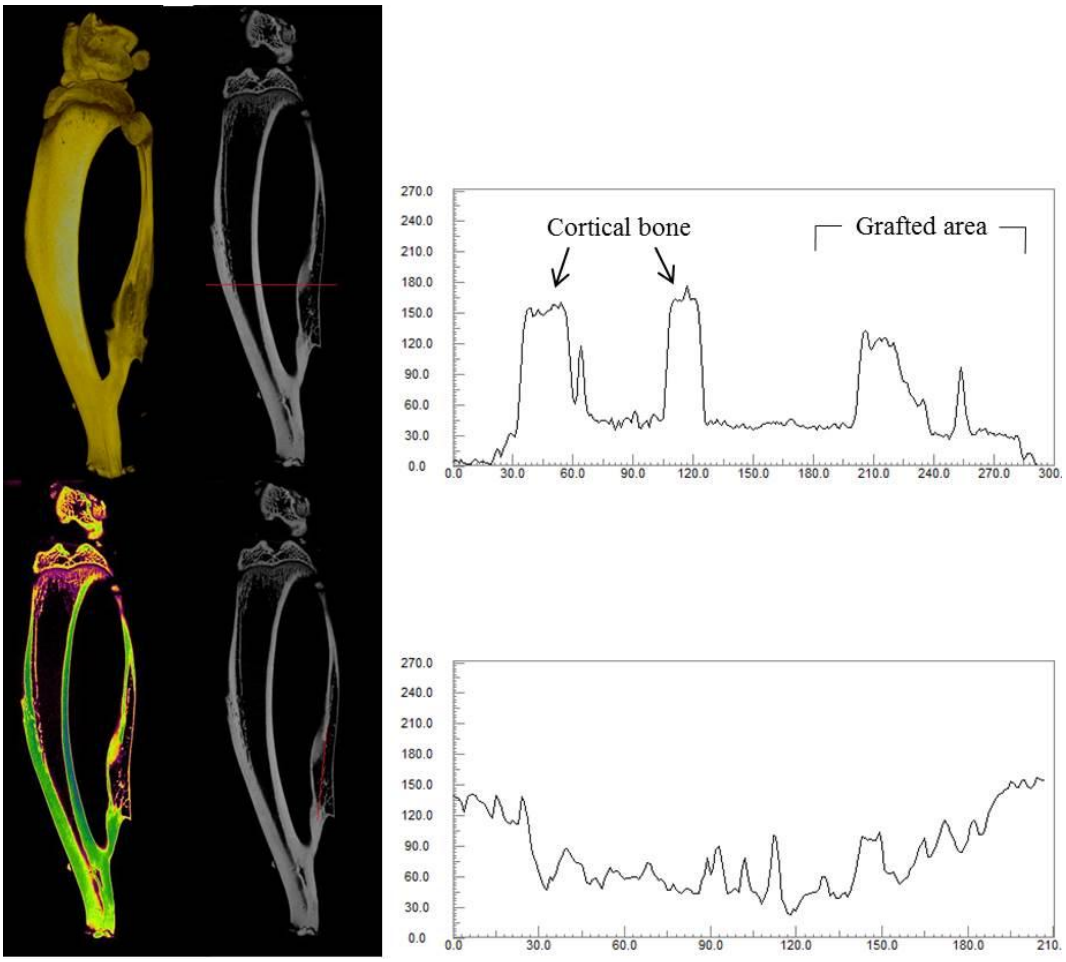

Figure 20. 3-dimensional reconstruction image, Long axis CT view of 8-week left fibula in experiment 2. Bone density was measured along the red line. In graphs, x-axis means length (pixel), and y-axis means bone density (Hounsfield unit).

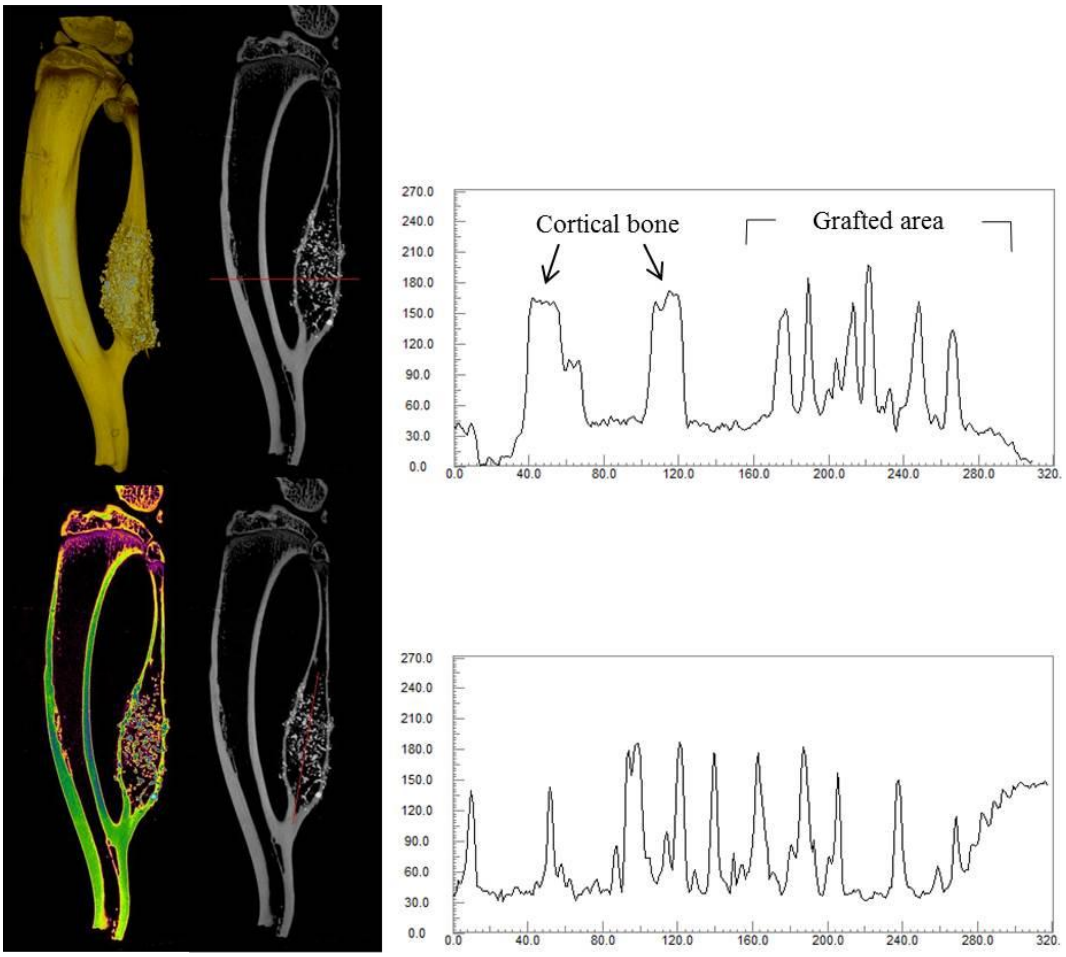

Figure 21. 3-dimensional reconstruction image, Long axis CT view of 8-week right fibula in experiment 2. Bone density was measured along the red line. In graphs, x-axis means length (pixel), and y-axis means bone density (Hounsfield unit).

3.4. Statistical analysis of micro-CT data

The average micro-CT values for each experimental group are presented in Figures 22–24 and Tables 3-6.

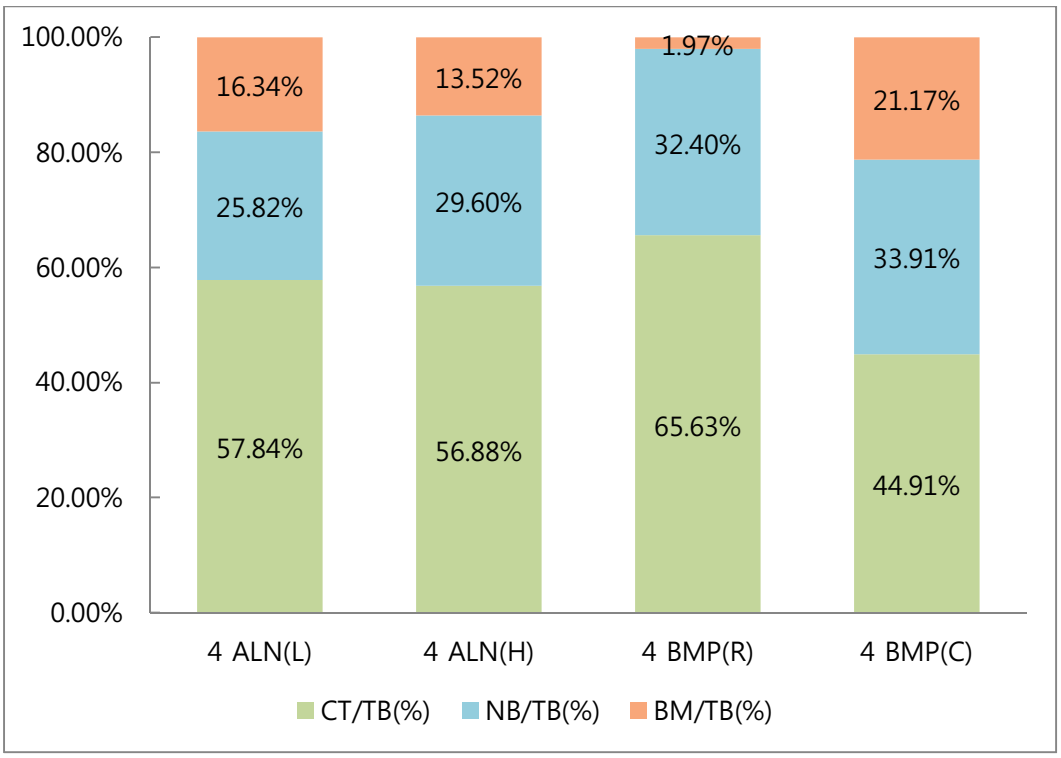

Figure 22. The rate of CT, NB, BM of 4-week experimental group. CT, connective tissue; NB, new bone; BM, bone material; TB, total bone; 4 ALN(L), low alendronate group of 4 weeks; 4 ALN(H), high alendronate group of 4 weeks; 4 BMP(R), rhBMP-2 group with Rapiderm pad® of 4 weeks; 4 BMP(C), rhBMP-2 group with CollaOss® of 4 weeks.

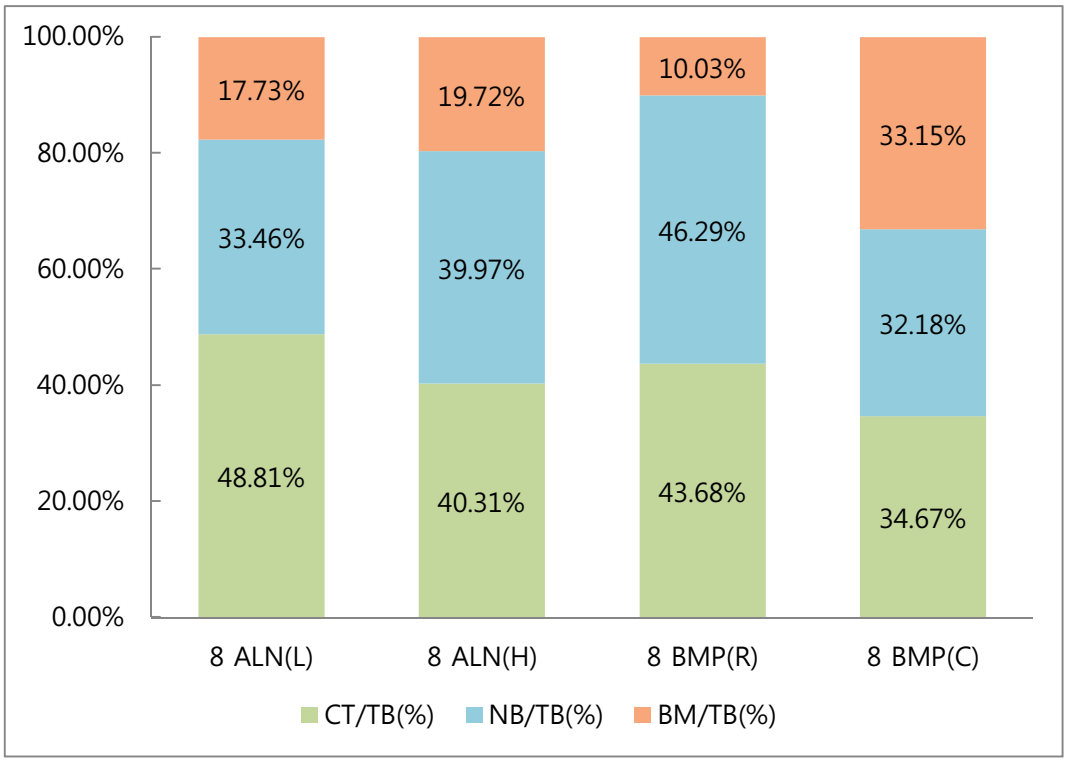

Figure 23. The rate of CT, NB, BM of 8-week experimental group. CT, connective tissue; NB, new bone; BM, bone material; TB, total bone; 8 ALN(L), low alendronate group of 8 weeks; 8 ALN(H), high alendronate group of 8 weeks; 8 BMP(R), rhBMP-2 group with Rapiderm pad® of 8 weeks; 8 BMP(C), rhBMP-2 group with CollaOss® of 8 weeks.

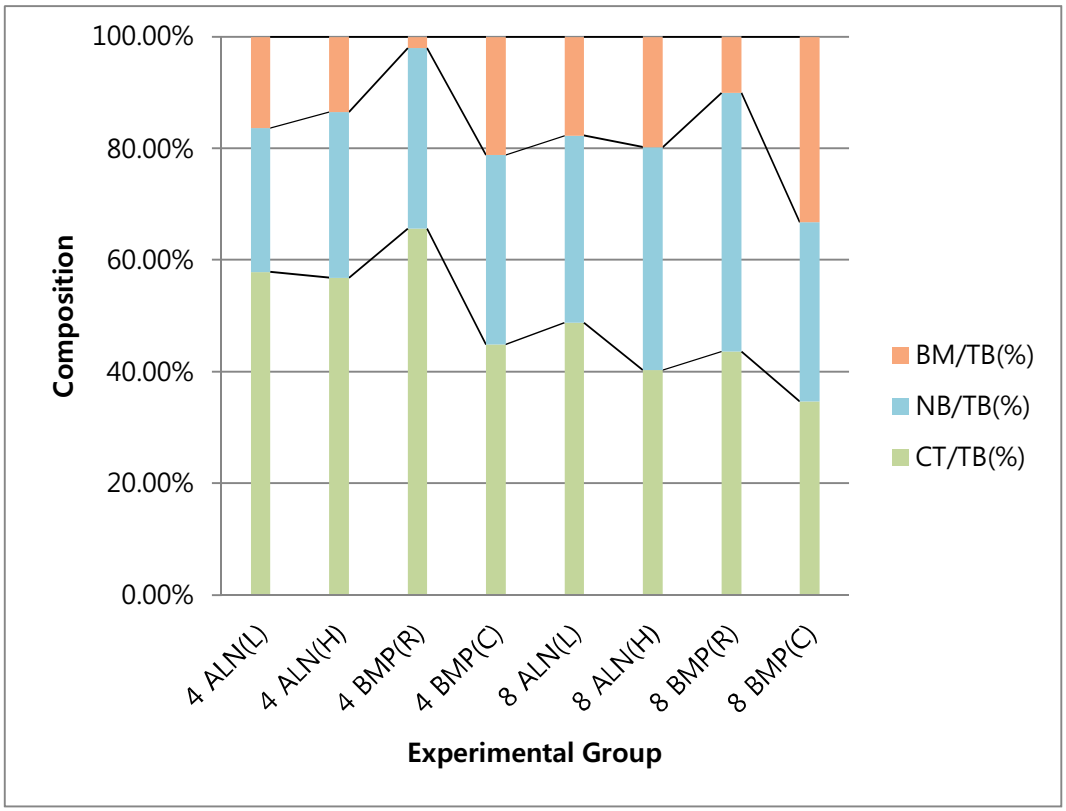

Figure 24. The rate of CT, NB, BM of 4 and 8-week experimental group. CT, connective tissue; NB, new bone; BM, bone material; TB, total bone; 4 ALN(L), low alendronate group of 4 weeks; 4 ALN(H), high alendronate group of 4 weeks; 4 BMP(R), rhBMP-2 group with Rapiderm pad® of 4 weeks; 4 BMP(C), rhBMP-2 group with CollaOss® of 4 weeks; 8 ALN(L), low alendronate group of 8 weeks; 8 ALN(H), high alendronate group of 8 weeks; 8 BMP(R), rhBMP-2 group with Rapiderm pad® of 8 weeks; 8 BMP(C), rhBMP-2 group with CollaOss® of 8 weeks.

Table 3. Statistical analysis of 4-week experimental group.

	TB/TV (%)		CT/TB (%)		NB/TB (%)		BM/TB (%)	
4 ALN(L) & 4 ALN(H)	70.37	.234	57.84	.505	25.82	.028*	16.34	003*
	61.71		56.88		29.60		13.52	
4 BMP(R) & 4 BMP(C)	27.08	.000*	65.63	.000*	32.40	.959	1.97	000*
	79.72		44.91		33.91		21.17	

* $p < 0.05$

Table 4. Statistical analysis of 8-week experimental group.

	TB/TV (%)		CT/TB (%)		NB/TB (%)		BM/TB (%)	
8 ALN(L) & 8 ALN(H)	64.99	.130	48.81	.003*	33.46	.007*	17.73	.328
	57.79		40.31		39.97		19.72	
8 BMP(R) & 8 BMP(C)	21.60	.000*	43.68	.000*	46.29	.000*	10.03	.000*
	75.95		34.67		32.18		33.15	

* $p < 0.05$

Table 5. Statistical analysis of 4 and 8-week experimental group.

	TB/TV		CT/TB		NB/TB		BM/TB	
4 ALN(L) & 8 ALN(L)	70.37	.328	57.84	.007*	25.82	.003*	16.34	.505
	64.99		48.81		33.46		17.73	
4 ALN(H) & 8 ALN(H)	61.71	.721	56.88	.000*	29.60	.000*	13.52	.003*
	57.79		40.31		39.97		19.72	
4 BMP(R) & 8 BMP(R)	27.08	.007*	65.63	.000*	32.40	.000*	1.97	.000*
	21.60		43.68		46.29		10.03	
4 BMP(C) & 8 BMP(C)	79.72	.442	44.91	.000*	33.91	.234	21.17	.001*
	75.95		34.67		32.18		33.15	

* $p < 0.05$

Table 6. Statistical analysis of ALN(H) and BMP(C) group.

	TB/TV		CT/TB		NB/TB		BM/TB	
4 ALN(H) & 4 BMP(C)	61.71	.015*	56.88	.001*	29.60	.065	13.52	.003*
	79.72		44.91		33.91		21.17	
8 ALN(H) & 8 BMP(C)	57.79	.001*	40.31	.005*	39.97	.000*	19.72	.000*
	75.95		34.67		32.18		33.15	

* $p < 0.05$

3.5. Histological findings

3.5.1. Experiment 1

In both the left and right fibulae at 4 weeks, histological analysis confirmed the continuity of the defect and graft areas in low-magnification images. Notably, for the right fibula, the new bone area was larger, and more bone materials remained in the defect area. In the left and right fibulae, osteocytes in new bone, osteoblasts, and multinucleate osteoclasts were arranged along the margin of new bone, as observed in high-magnification images. Inflammation was observed in both defect areas in the left and right fibula, with greater inflammation found in the right fibula, in which a higher concentration of alendronate was used (Figure 25 and 26).

Interestingly, at 8 weeks, increased bone formation and reduced inflammatory cell infiltration were observed in the left fibula. Increased M-T staining, representative of bone tissue, was also observed at the center of the grafted area, and the amount of remaining bone material was reduced compared with that at 4 weeks (Figure 27). In contrast, little remaining bone material was observed, without dense inflammatory cell areas in the right fibula. We also observed osteoblasts and osteoclasts along the newly formed bone (Figure 28).

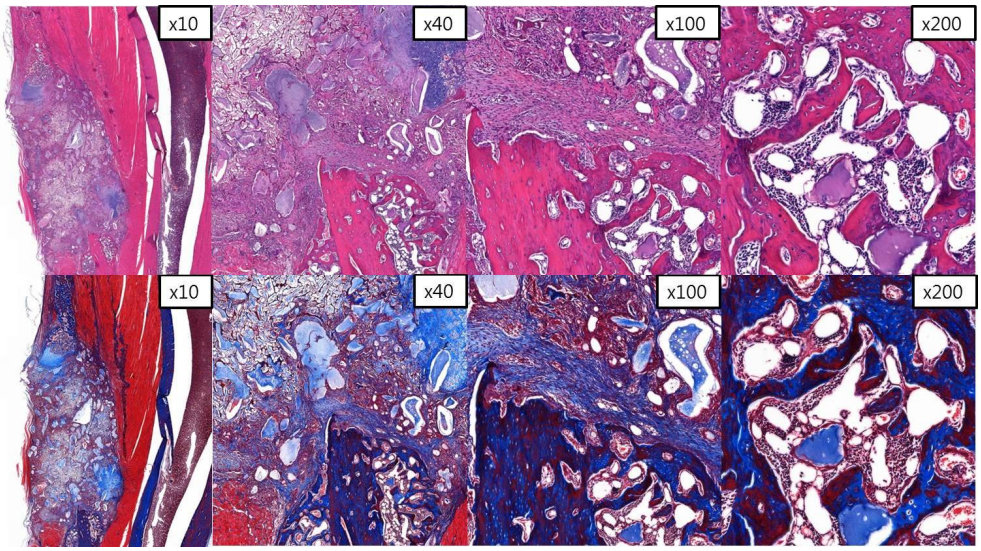

Figure 25. Histologic findings of 4-week left fibula in experiment 1. Newly formed bone and inflammatory cells were observed. (Hematoxylin and eosin (*above*), Masson-Trichrome (*below*))

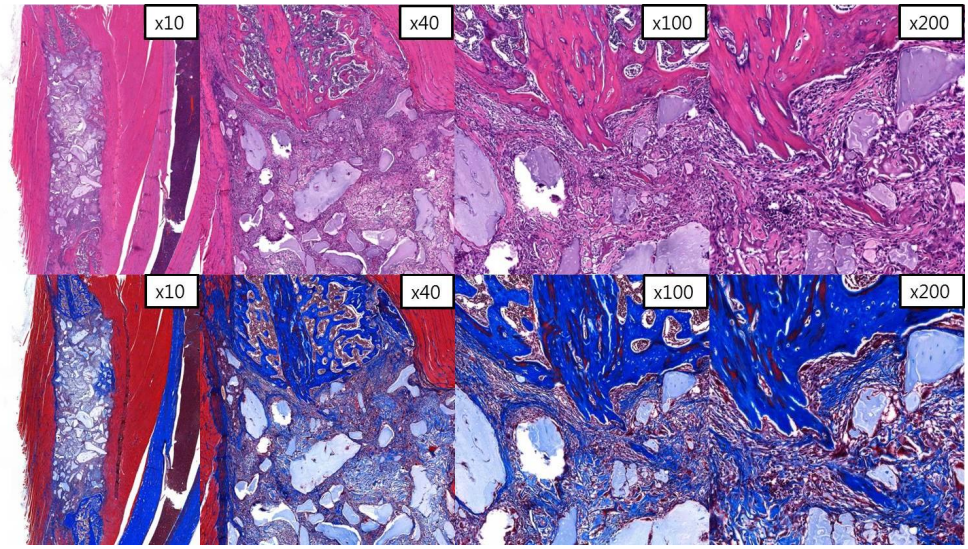

Figure 26. Histologic findings of 4-week right fibula in experiment 1. Newly formed bone and inflammatory cells were observed. (Hematoxylin and eosin (*above*), Masson-Trichrome (*below*))

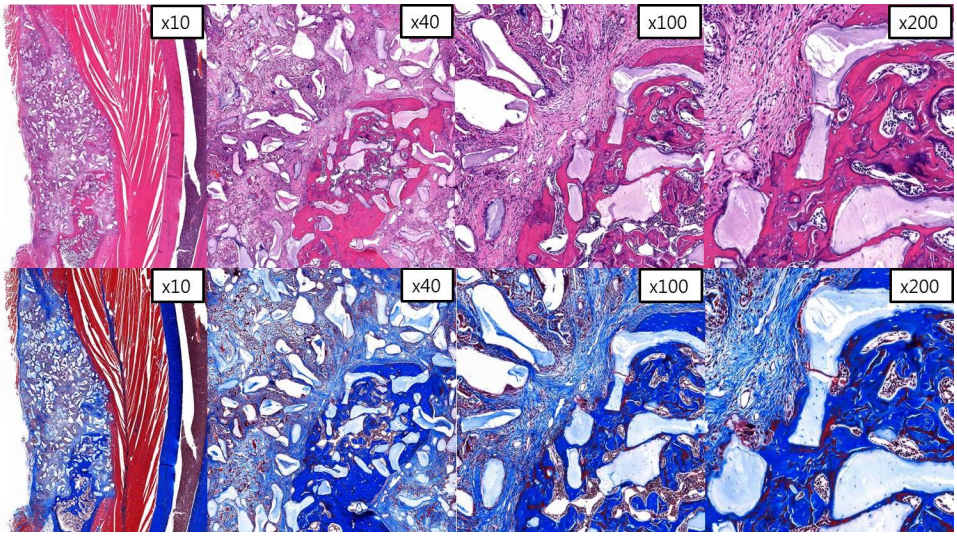

Figure 27. Histologic findings of 8-week left fibula in experiment 1. Increased bone formation and reduced inflammatory cell infiltration were observed than 4-week group. (Hematoxylin and eosin (*above*), Masson-Trichrome (*below*))

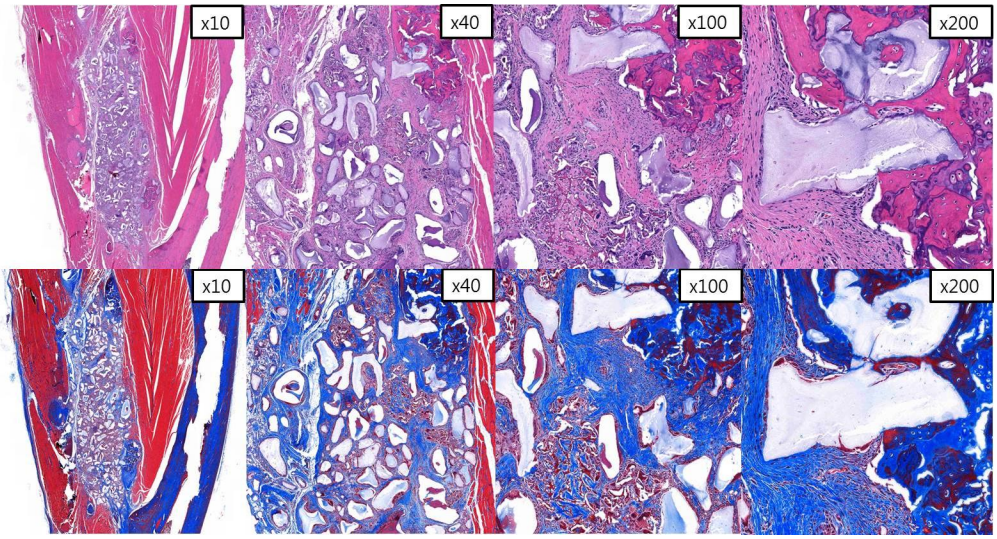

Figure 28. Histologic findings of 8-week right fibula in experiment 1. The area of remaining bone material was smaller than 4-week group. Osteoblasts and osteoclasts along the newly formed bone were observed. (Hematoxylin and eosin (*above*), Masson-Trichrome (*below*))

3.5.2. Experiment 2

At 4 weeks, more prominent continuous new bone formation was observed in the left fibula in experiment 2, in which rhBMP-2 was used, compared with that in experiment 1, in which alendronate was used without rhBMP-2. The formation of the cortical layer was observed for both the proximal and distal sides, and abundant fatty marrow, osteocytes, osteoblasts, and osteoclasts were observed in the left fibula (Figure 29). In contrast, the thickness of the cortex was reduced in the right fibula compared with that in the left fibula. However, the use of the xenogenic bone promoted greater new bone formation at the center of the grafted area than observed for the absorbable collagen. Moreover, similar to the left fibula, plenty of fatty marrow, osteocytes, osteoblasts, and osteoclasts were observed in the right fibula, located in the margin or new bone (Figure 30).

At 8 weeks, greater regeneration of bone in the inner grafted area was observed relative to that at 4 weeks for both the left and right fibulae. In the left fibula, the thickness of the cortex layer was greater, and a lamellar bone appearance was noted. New bone formation in the segmental defect area and cortex was greater in the left fibula than in the right fibula (Figure 31). However, gross analysis suggested that new bone formation was highest in the right fibula at 8 weeks. Less bone graft material remained in the right fibula, and bone material had been replaced with new bone and fatty marrow (Figure 32).

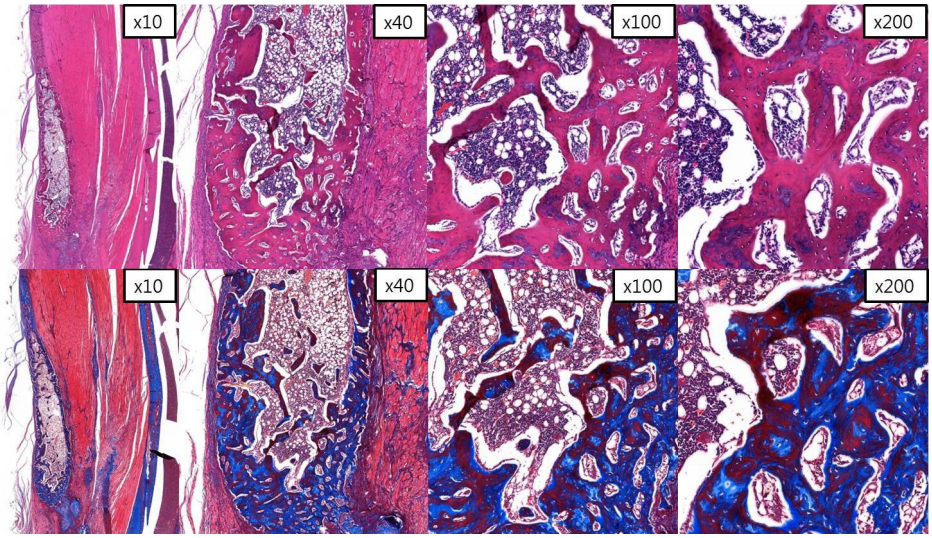

Figure 29. Histologic findings of 4-week left fibula in experiment 2. Fatty marrow, osteocytes, osteoblasts, and osteoclasts were observed. (Hematoxylin and eosin (*above*), Masson-Trichrome (*below*))

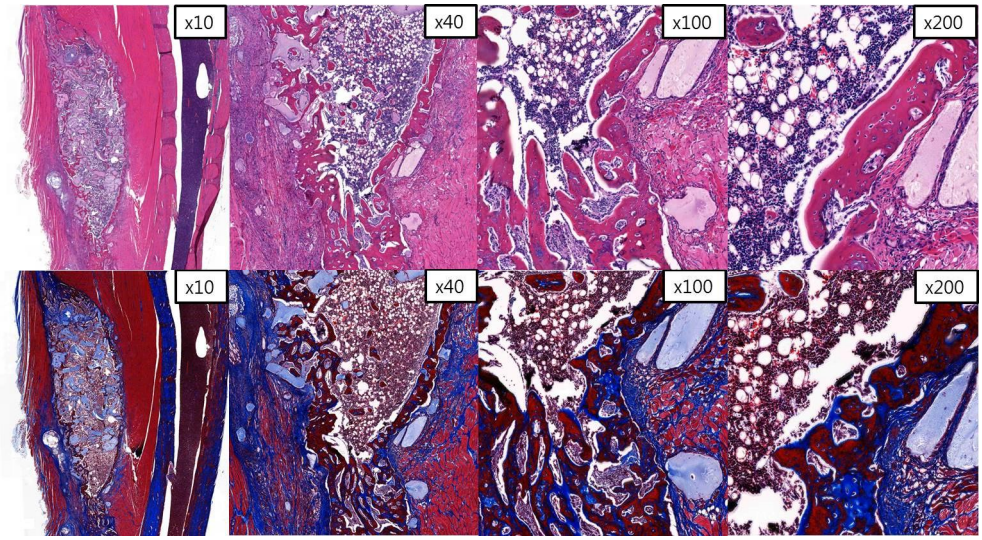

Figure 30. Histologic findings of 4-week right fibula in experiment 2. The grafted area was consisted with plenty of fatty marrow, osteocytes, osteoblasts, and osteoclasts. Some of remaining bone material was also observed. (Hematoxylin and eosin (*above*), Masson-Trichrome (*below*))

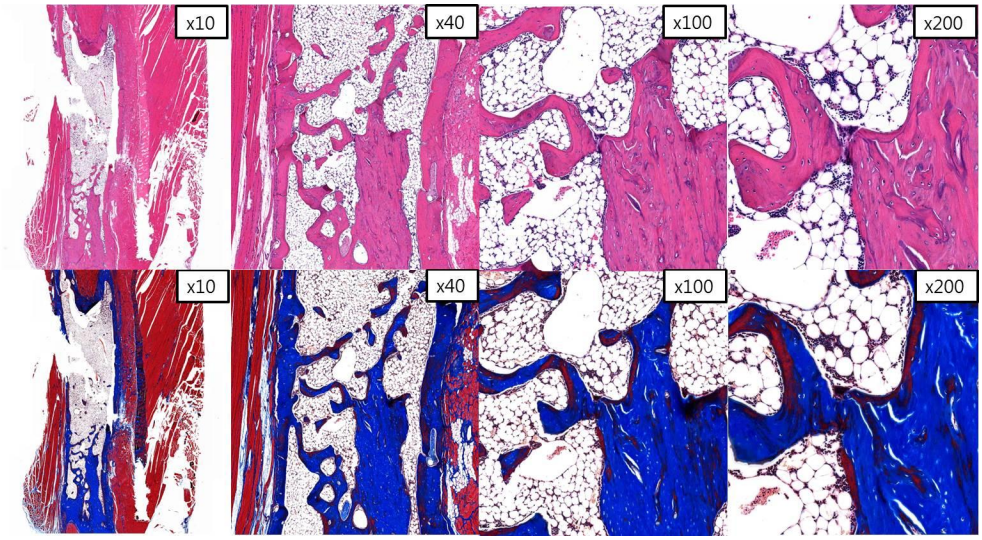

Figure 31. Histologic findings of 8-week left fibula in experiment 2. New bone formation in the segmental defect area and cortex was greater than 4-week group. (Hematoxylin and eosin (*above*), Masson-Trichrome (*below*))

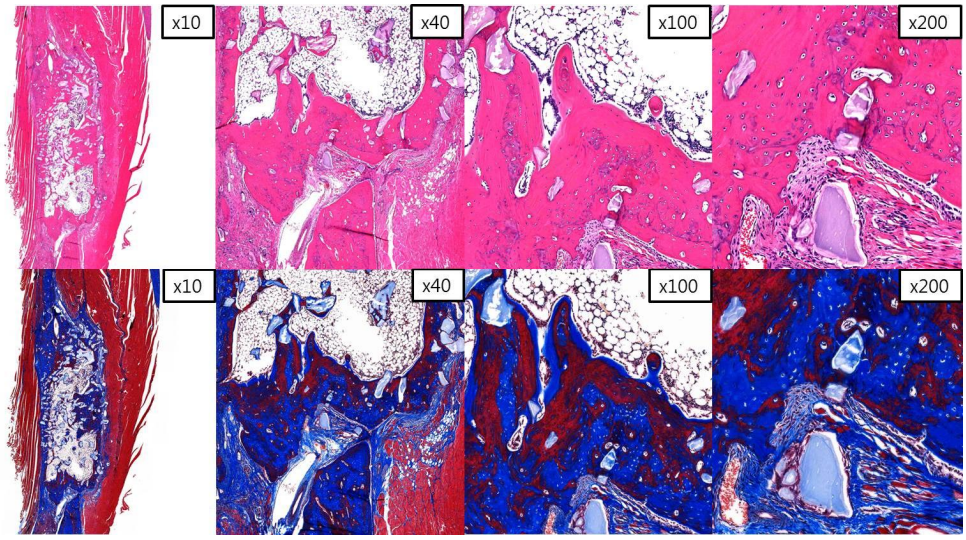

Figure 32. Histologic findings of 8-week right fibula in experiment 2. The area of remaining graft material was smaller than 4-week group. Grafted bone material was replaced with new bone and fatty marrow. (Hematoxylin and eosin (*above*), Masson-Trichrome (*below*))

3.6. Histomorphometric analysis

Histomorphometric analysis showed that proximal bone formation was significantly higher in the rhBMP-2 group with the xenogenic bone than in all other experimental groups. Adipose tissue was observed only in the rhBMP-2 group (Figure 33). The thickness of the cortical layer for the absorbable collagen group was similar to but slightly greater than that of the xenogenic bone graft group (Figure 34).

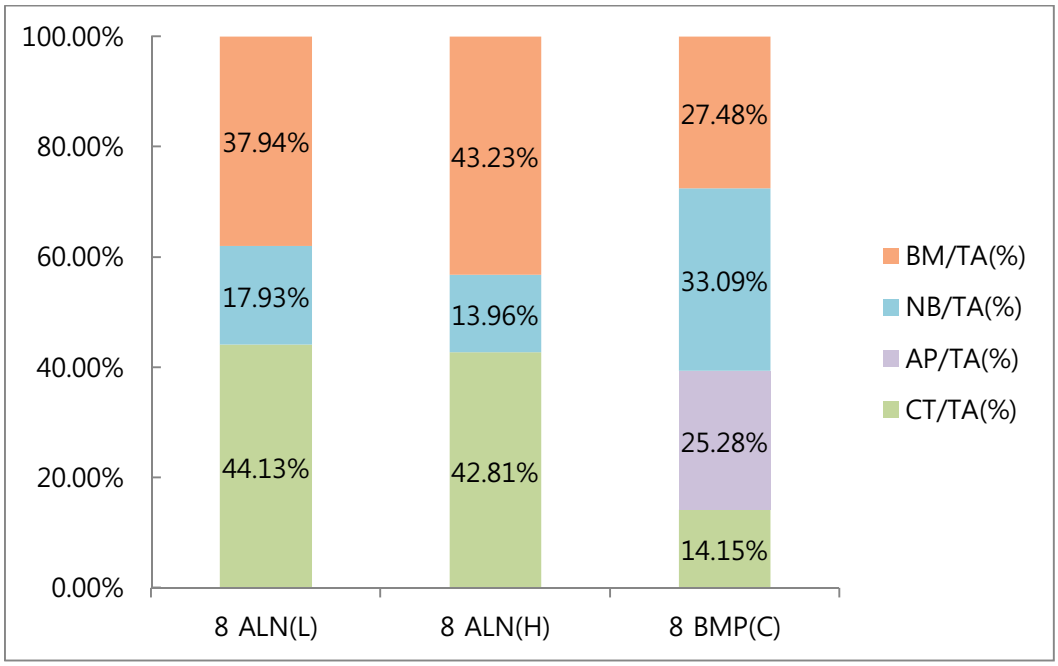

Figure 33. The rate of CT, AP, NB, BM of 8-week experimental group. CT, connective tissue; AP, adipose tissue; NB, new bone; BM, bone material; TA, total area; 8 ALN(L), low alendronate group of 8 weeks; 8 ALN(H), high alendronate group of 8 weeks; 8 BMP(C), rhBMP-2 group with CollaOss® of 8 weeks.

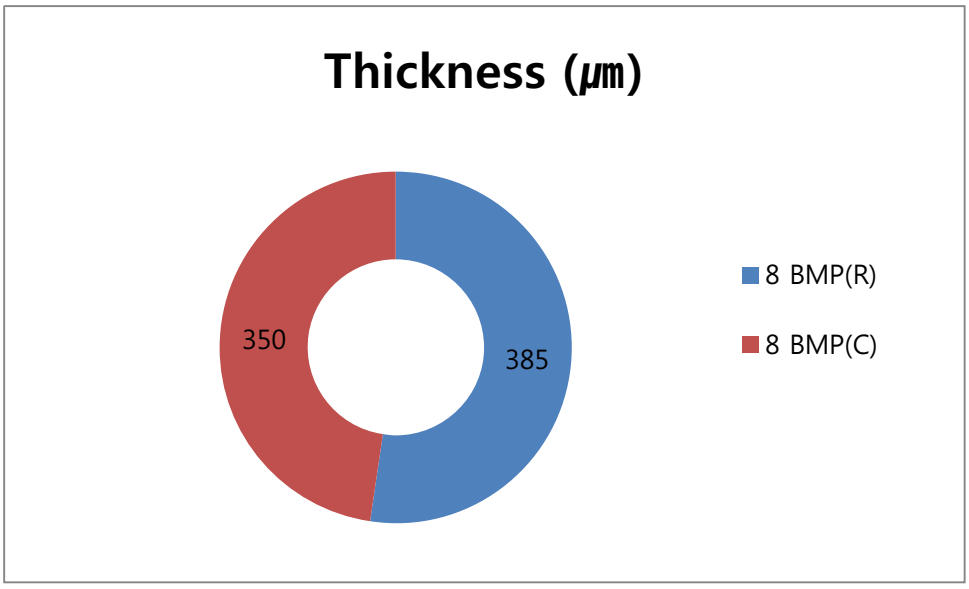

Figure 34. The thickness of cortical layer of 8-week experimental group.

3.7. Immunohistochemical findings

Immunohistochemical analysis showed that BMP2 exhibited weak to moderate expression in the left and right fibulae in experiment 1 at 4 weeks. BMP2 expression was increased in the margin of newly formed bone for both the left and right fibulae at 8 weeks (Figure 35). Similar results were observed in experiment 2, with higher expression of BMP2 at 8 weeks (Figure 36). In contrast, for OPG, there were no differences among groups at 4 weeks, and only weak expression was observed at 8 weeks for both experiments 1 and 2 (Figures 37 and 38).

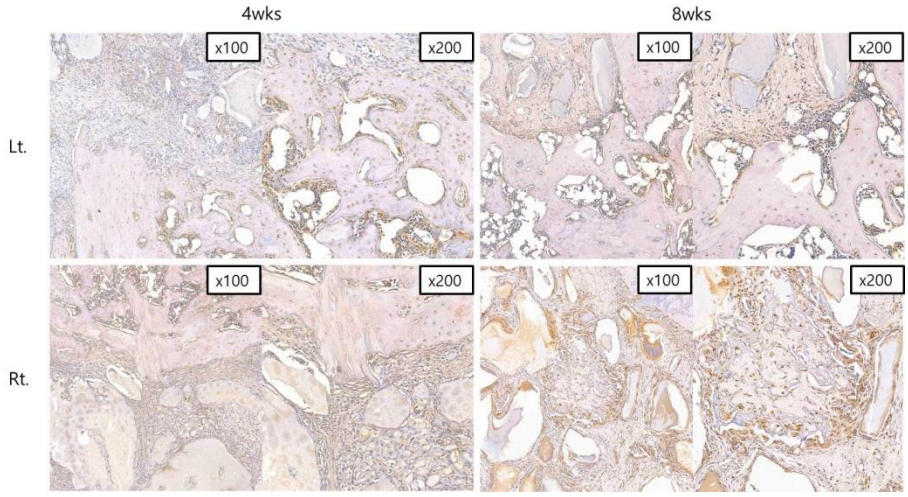

Figure 35. Immunohistochemical findings with BMP2 of experimental group 1. BMP2 expression was increased in the margin of newly formed bone in both the left and right fibulae at 8 weeks.

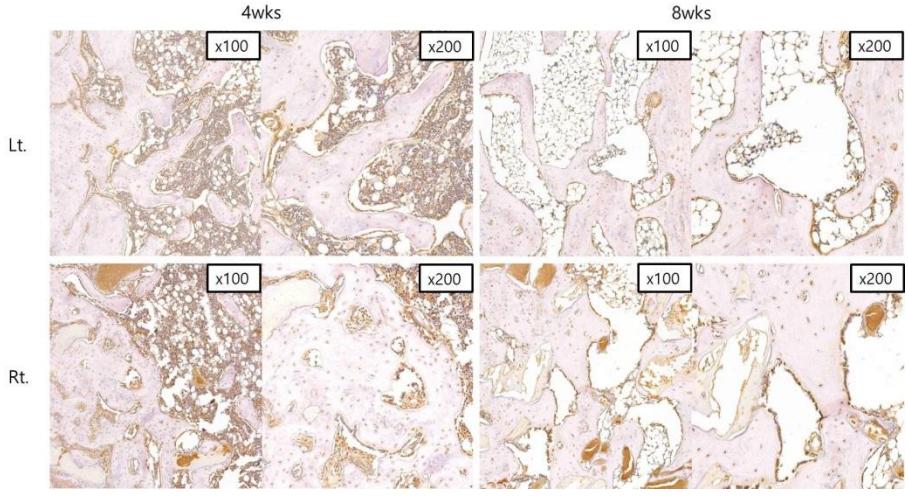

Figure 36. Immunohistochemical findings with BMP2 of experimental group 2. BMP2 expression was increased in the margin of newly formed bone in both the left and right fibulae at 8 weeks.

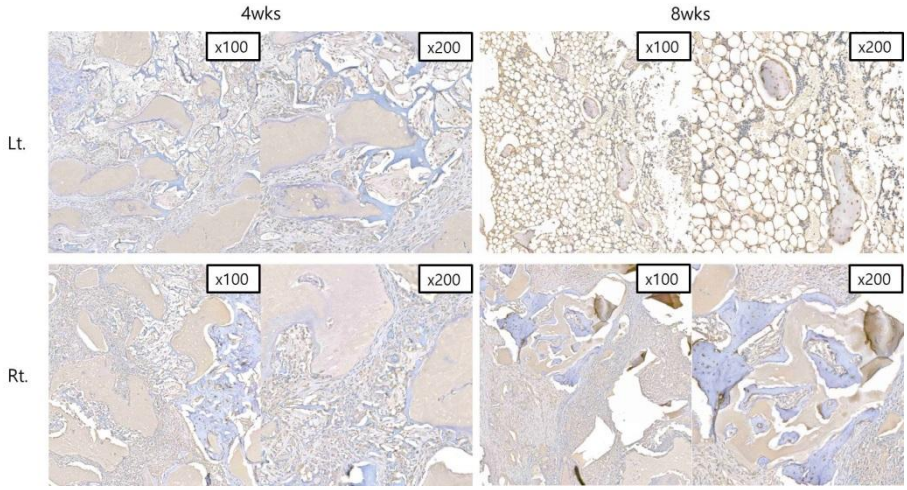

Figure 37. Immunohistochemical findings with OPG of experimental group 1. No OPG expression was found in 4-week group. Weak expression was observed in 8-week group.

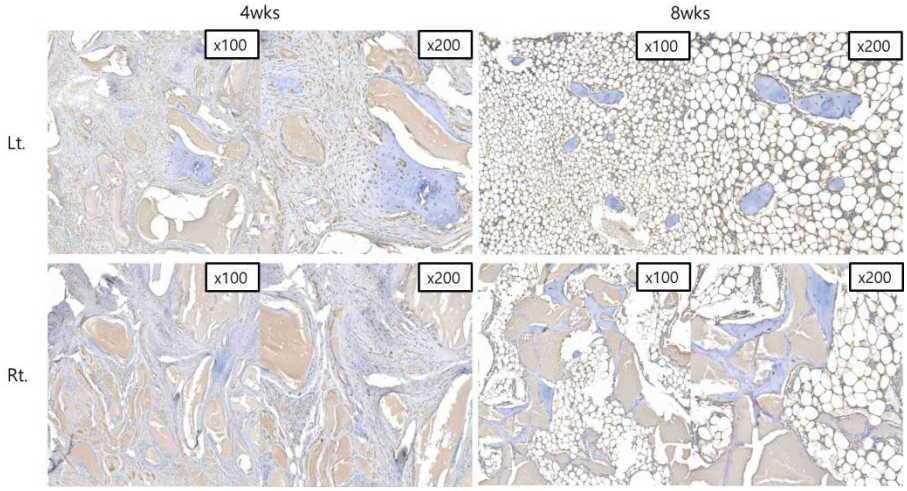

Figure 38. Immunohistochemical findings with OPG of experimental group 2. No OPG expression was found in 4-week group. Weak expression was observed in 8-week group.

4. Discussion

Bone remodeling is result of turnover between osteoblasts and osteoclasts, which synthesize and remove the bone tissue (Vaananen, 1993). Bisphosphonate is a pyrophosphate analog in which the central oxygen atom of pyrophosphate is substituted with carbon. The side chains with this carbon atom confer the molecule with various antiresorptive effects (Ramaswamy and Shapiro, 2003). Nitrogen-containing bisphosphonates inhibit the mevalonate pathway by preventing farnesyl diphosphate synthase (Gong et al., 2011). The mevalonate pathway functions to synthesize cholesterol and isoprenoid lipids. By blocking the mevalonate pathway, nitrogen-containing bisphosphonate exerts potent antiresorptive effects. Bisphosphonates are widely used as a first-line treatment for osteoporosis (Grey and Reid, 2006), preventing bone fracture. Additionally, bisphosphonates have been exploited for their antiproliferative and pro-apoptotic effects on tumor cells and have been used for the treatment of Paget's disease, breast cancer, bone metastasis, multiple myeloma, and primary hyperparathyroidism (Baykan et al., 2014; Khan et al., 2009; Pavlakis et al., 2005). As the prevalence of osteoporosis has increased, the number of patients suffering from bisphosphonate-associated osteonecrosis of the jaw (BRONJ) has also increased. Marx et al. (2007) highlighted concerns regarding the use of bisphosphonate in dentistry. Moreover, medication-related osteonecrosis of the jaw (MRONJ) has been described by the American Association of Oral and Maxillofacial Surgeons (Ruggiero et al., 2014).

Despite these concerns, the alendronate has been shown to stimulate osteogenic differentiation of mesenchymal cells (Lindtner et al., 2014). Other studies have shown that alendronates enhance bone formation in repair of critical sized calvarial defects (Toker et al., 2012; Wang et al., 2010). Furthermore, a recent study used bisphosphonates locally to facilitate new bone formation because of the effects of bisphosphonates on inhibition of osteoclast activity and promotion of osteoblast differentiation (Malavasi et al., 2016). However, no previous studies had specifically evaluated the optimal concentration of alendronate. In previous studies, the concentration used to prevent root resorption in delayed replantation after extraction of teeth was 1 mM (0.325 mg/mL) (Kim et al., 2015; Komatsu et al., 2008; Levin et al., 2001; Shibata et al., 2004). Moreover, in another previous study (Kwon, 2011), 2.0 mg/mL alendronate with biphasic calcium phosphate (BCP) was shown to promote new bone formation, and xenogenic grafts were shown to promote osteoconduction, without evidence of osteoinduction in the defect area (Baek, 2013). Thus, in this study, we used two concentrations of alendronate, 1 mM and 10 mM. Our results showed dose-dependent effects on new bone formation in our rat model in vivo.

Our micro-CT data showed prominent new bone formation and higher rates of remaining bone material when the higher concentration of alendronate was used. These results may be related to reduced osteoclast activity and anabolic effects of osteoblast differentiation. In contrast, histomorphometric analysis revealed that the rate of new bone formation was relatively low in the high-concentration alendronate group compared with

that in the low-concentration alendronate group. However, histomorphometric findings only showed the end of the resection margin, whereas some new bone formation was observed in the center of the grafted area in specimens treated with a higher concentration of alendronate. In macroscopic analysis, which included all of the grafted area, the connective tissue was significantly decreased, whereas new bone was increased in the high-concentration group. Accordingly, although the low concentration (1 mM) was suitable for preventing root resorption, 10 mM was required for regenerating bone when administered locally.

rhBMP-2 is a strong osteoinductive factor and induces the differentiation of mesenchymal stem cells into osteogenic cells to accelerate new bone formation (Turgeman et al., 2002). Many studies have demonstrated the efficacy of rhBMP-2, including its utility for maxillary sinus augmentation and in large primary bone defect areas (Kim et al., 2015). Moreover, rhBMP-2 may enhance new bone formation. However, no appropriate carriers that can function as scaffolds and then be resorbed and replaced with newly formed bone. In our analysis, we examined and compared rhBMP-2 with xenogenic bone and absorbable collagen sponges. Our results showed that the xenogenic bone was not superior to the sponges in terms of new bone formation at 4 or 8 weeks. For reconstruction of large defect areas, such as segmental mandibulectomy, osteogenic and osteoinductive graft materials and carriers having the appropriate strength and scaffold function during certain periods of healing are critical for achieving a favorable prognosis. Xenogenic bone has good strength, but the remaining bone material is not well absorbed.

On the other hand, absorbable collagen is a useful carrier for new bone formation, but does not exhibit sufficient mechanical strength. Notably, in our study, our findings showed that the absorbable sponge resulted in increased thickness of the cortical layer and increased density of the cortex compared with the results in the xenogenic bone group. Therefore, when using rhBMP-2, the absorbable collagen sponge could act as an effective carrier. Further studies are needed to better characterize the effects of absorbable sponges and xenogenic bone on new bone formation.

In this study, we observed new bone formation by histomorphometric analysis at 8 weeks in rhBMP-2 treated specimens, particularly at the end of the resected margin. However, when analyzing the whole grafted area by micro-CT, higher rates of bone formation and lower rates of remaining bone graft material were observed when a higher concentration of alendronate was used along with rhBMP-2. Micro-CT data were calculated using HU; thus, it is possible that newly formed bone may have been harder than the upper limit. Although micro-CT cannot be directly visualized, it is more reliable because it allows gross volume analysis. Based on these considerations, our findings support that locally administered bisphosphonate effectively promoted new bone formation when combined with rhBMP-2.

Immunohistochemistry analysis confirmed strong expression of BMP2 in our samples. Moreover, the increased expression of BMP2 relative to that of OPG highlighted the higher activity of osteoblasts relative to that of osteoclasts. OPG is an important regulator of osteoclastogenesis that functions by binding to RANK and inhibiting bone resorption

(Boyce and Xing, 2007; Kohli and Kohli, 2011; Perez-Sayans et al., 2010). However, we did not observe high expression of OPG in this study. Some other studies have shown that alendronate does not affect OPG gene expression but may be related to RANKL gene expression (Enjuanes et al., 2010).

5. Conclusion

In this study, our results showed optimal reconstruction of the resected area by grafting with absorbable collagen sponges containing rhBMP-2. However, in intraoral segmental defect, grafted material bears the mastication force. Therefore, the future researches are needed to draw a conclusion of time for keeping excellent stability and strength. Local administration of bisphosphonate was also shown to be beneficial for new bone formation. However, further studies are needed to determine the optimal alendronate concentration and hardening time. Moreover, the use of bisphosphonate as an inducible agent would require cellular level studies of the mechanisms of bone formation. Finally, many studies have examined the possibility of using customized scaffold to replace large bone defects (Ciocca et al., 2013). Thus, in the future, it will be necessary to fabricate customized scaffolds that are porous and absorbable and can provide sufficient control of the release of osteoinductive components using gene therapy, tissue engineering, and 3D bioprinting approaches.

6. References

Baek JW: The effect of bone regeneration and changes of microstructures in a segmental defect using collagen-combined xenogenic bone and rhBMP-2 in the SD rat fibula. The Graduate School of Yonsei University, Korea, 2013.

Baykan EK, Saygili LF, Erdogan M, Cetinkalp S, Ozgen AG, Yilmaz C: Efficacy of zoledronic acid treatment in Paget disease of bone. *Osteoporos Int* 25(9): 2221-2223, 2014.

Boyce BF, Xing L: Biology of RANK, RANKL, and osteoprotegerin. *Arthritis Res Ther* 9 Suppl 1: S1, 2007.

Ciocca L, Donati D, Ragazzini S, Dozza B, Rossi F, Fantini M, et al.: Mesenchymal stem cells and platelet gel improve bone deposition within CAD-CAM custom-made ceramic HA scaffolds for condyle substitution. *Biomed Res Int* 2013: 549762, 2013.

Enjuanes A, Ruiz-Gaspa S, Peris P, Ozalla D, Alvarez L, Combalia A, et al.: The effect of the alendronate on OPG/RANKL system in differentiated primary human osteoblasts. *Endocrine* 37(2): 322-328, 2010.

Gong L, Altman RB, Klein TE: Bisphosphonates pathway. *Pharmacogenet Genomics* 21(1): 50-53, 2011.

Grey A, Reid IR: Differences between the bisphosphonates for the prevention and treatment of osteoporosis. *Ther Clin Risk Manag* 2(1): 77-86, 2006.

Hollinger JO, Kleinschmidt JC: The critical size defect as an experimental model to test bone repair materials. *J Craniofac Surg* 1(1): 60-68, 1990.

Khan A, Grey A, Shoback D: Medical management of asymptomatic primary hyperparathyroidism: proceedings of the third international workshop. *J Clin Endocrinol Metab* 94(2): 373-381, 2009.

Kim HC, Song JM, Kim CJ, Yoon SY, Kim IR, Park BS, et al.: Combined effect of bisphosphonate and recombinant human bone morphogenetic protein 2 on bone healing of rat calvarial defects. *Maxillofac Plast Reconstr Surg* 37(1): 16, 2015.

Kim HJ, Chung JH, Shin SY, Shin SI, Kye SB, Kim NK, et al.: Efficacy of rhBMP-2/Hydroxyapatite on Sinus Floor Augmentation: A Multicenter, Randomized Controlled Clinical Trial. *J Dent Res* 94(9 Suppl): 158s-165s, 2015.

Kohli SS, Kohli VS: Role of RANKL-RANK/osteoprotegerin molecular complex in bone remodeling and its immunopathologic implications. *Indian J Endocrinol Metab* 15(3): 175-181, 2011.

Komatsu K, Shimada A, Shibata T, Shimoda S, Oida S, Kawasaki K, et al.: Long-term effects of local pretreatment with alendronate on healing of replanted rat teeth. *J Periodontal Res* 43(2): 194-200, 2008.

Kwon JI: Effect of locally administered bisphosphonate on bone regeneration and micro-architecture in segmental defect in the SD rat fibula. The Graduate School of Yonsei University, Korea, 2011.

Levin L, Bryson EC, Caplan D, Trope M: Effect of topical alendronate on root resorption of dried replanted dog teeth. *Dent Traumatol* 17(3): 120-126, 2001.

Lindtner RA, Tiaden AN, Genelin K, Ebner HL, Manzl C, Klawitter M, et al.: Osteoanabolic effect of alendronate and zoledronate on bone marrow stromal cells (BMSCs) isolated from aged female osteoporotic patients and its implications for their mode of action in the treatment of age-related bone loss. *Osteoporos Int* 25(3): 1151-1161, 2014.

Malavasi M, Louro R, Barros MB, Teixeira LN, Peruzzo DC, Joly JC, et al.: Effects of risedronate on osteoblastic cell cultures. *Arch Oral Biol* 68: 43-47, 2016.

Marx RE, Cillo JE, Jr., Ulloa JJ: Oral bisphosphonate-induced osteonecrosis: risk factors, prediction of risk using serum CTX testing, prevention, and treatment. *J Oral Maxillofac Surg* 65(12): 2397-2410, 2007.

Park SH: Bone regeneration in a critical sized segmental defect in the SD rat fibula using a ErhBMP-2/ACS implant. The Graduate School of Yonsei University, Korea, 2010.

Pavlakis N, Schmidt R, Stockler M: Bisphosphonates for breast cancer. *Cochrane Database Syst Rev* (3): Cd003474, 2005.

Perez-Sayans M, Somoza-Martin JM, Barros-Angueira F, Rey JM, Garcia-Garcia A: RANK/RANKL/OPG role in distraction osteogenesis. *Oral Surg Oral Med Oral Pathol Oral Radiol Endod* 109(5): 679-686, 2010.

Ramaswamy B, Shapiro CL: Bisphosphonates in the prevention and treatment of bone metastases. *Oncology (Williston Park)* 17(9): 1261-1270; discussion 1270-1262, 1277-1268, 1280, 2003.

Ruggiero SL, Dodson TB, Fantasia J, Goodday R, Aghaloo T, Mehrotra B, et al.: American Association of Oral and Maxillofacial Surgeons position paper on medication-related osteonecrosis of the jaw--2014 update. *J Oral Maxillofac Surg* 72(10): 1938-1956, 2014.

Schilephake H: Bone growth factors in maxillofacial skeletal reconstruction. *Int J Oral Maxillofac Surg* 31(5): 469-484, 2002.

Shibata T, Komatsu K, Shimada A, Shimoda S, Oida S, Kawasaki K, et al.: Effects of alendronate on restoration of biomechanical properties of periodontium in replanted rat molars. *J Periodontal Res* 39(6): 405-414, 2004.

Toker H, Ozdemir H, Ozer H, Eren K: Alendronate enhances osseous healing in a rat calvarial defect model. *Arch Oral Biol* 57(11): 1545-1550, 2012.

Turgeman G, Zilberman Y, Zhou S, Kelly P, Moutsatsos IK, Kharode YP, et al.: Systemically administered rhBMP-2 promotes MSC activity and reverses bone and cartilage loss in osteopenic mice. *J Cell Biochem* 86(3): 461-474, 2002.

Urist MR: Bone: formation by autoinduction. *Science* 150(3698): 893-899, 1965.

Vaananen HK: Mechanism of bone turnover. *Ann Med* 25(4): 353-359, 1993.

Wang CZ, Chen SM, Chen CH, Wang CK, Wang GJ, Chang JK, et al.: The effect of the local delivery of alendronate on human adipose-derived stem cell-based bone regeneration. *Biomaterials* 31(33): 8674-8683, 2010.

국문 요약

백서 비골 모델에서 bisphosphonate와 rhBMP-2의 국소 적용이 골 재생에 미치는 영향

연세대학교 대학원 치의학과
곽은정
지도교수: 김형준

구강악안면영역에 있어서 골 결손시 자가골, 이종골 및 합성골을 이용한 골 증강술이 활발히 시행되고 있고 이중 자가골을 이용한 재건이 가장 바람직하겠으나 종양이나 외상으로 인해 재건 부위가 클 경우 이종골 및 합성골 등의 골이식재의 사용이 불가피하다. 또한, 골 형성 인자 중 recombinant human bone morphogenic protein-2 (rhBMP-2) 는 환자의 골 치유 시 신생골 형성을 유도할 수 있는 인자로 알려져 있다. 신생골 형성에 있어 골 형성 인자 뿐만 아니라 carrier 또한 중요하지만 적절한 rhBMP-2의 carrier에 대한 연구가 부족하다. 또한 최근 적정 농도의 비스포스포네이트 제제가 골모세포에도 작용하여 골 재생을 유도할 수도 있다는 연구 결과가 발표되고 있다. 따라서 본 연구의 목적은 porcine bone 기원의 이종골과 흡수성 콜라겐 스펀지의 rhBMP-2 carrier로서의 역할과 함께 국소 적용된 비스포스포네이트가 골 치유에 미치는 영향을 웅성 백서 비골의 임계 크기 결손 모델에서 비교 관찰하기 위함이다.

실험은 8주령의 Sprague-Dawley 백서 32마리를 대상으로 하였으며 두 그룹으로 나누었다. 백서의 양측 비골에 약 7mm 임계 크기의 분절성 골 결손을 형성한 후 실험 1은 좌측에는 저농도의 비스포스포네이트를 적용한 이종골을,

우측에는 고농도의 비스포스포네이트를 적용한 이종골을 이식하였다. 실험 2는 좌측에는 흡수성 콜라겐 스펀지를, 우측에는 이종골을 rhBMP-2의 carrier로서 각각 사용하였다. 실험 4, 8주 후 희생하여 육안적, 방사선학적, 조직학적, 조직형태학적 및 면역조직화학적 분석을 시행하였다.

고농도의 비스포스포네이트 실험군에서는 저농도의 경우보다 더 많은 신생골 형성 소견이 관찰되었다. 또한 rhBMP-2는 흡수성 콜라겐 스펀지와 이종골을 사용한 실험 모두에서 골 결손부와 이식재 사이 연속성이 관찰되었다. 새로 형성된 피질골의 두께는 특히 8주차 흡수성 콜라겐 스펀지 실험군에서 기존 비골과 유사한 소견을 보였다. 또한, 고농도 비스포스포네이트 실험군에서 rhBMP-2 실험군에 조금 못 미치지만 우수한 골형성능을 보였다.

결론적으로 국소 적용된 비스포스포네이트는 신생골 형성을 촉진하고 특히 고농도에서 저농도보다 골형성이 많이 이루어졌다. 흡수성 콜라겐 스펀지는 골이식재가 남지 않고 기존 비골과 유사한 형태로 재형성된다는 장점이 있었다. 이들 골이식재 및 골 형성 인자들이 기존 골을 완전히 대체하기 위해서는 안정성과 기계적 강도에 관한 추가 연구가 필요할 것이다.

핵심되는 말 : 비스포스포네이트, rhBMP-2, 골형성, 이종골 이식, 흡수성 콜라겐 스펀지